Life Sciences 84 (2009) 876–881

Contents lists available at ScienceDirect

Life Sciences

journal homepage: www.elsevier.com/locate/lifescie

Effects of long-term dipeptidyl peptidase-IV inhibition on body composition and glucose tolerance in high fat diet-fed mice

Xibao Liu [a], Norio Harada [a], Shunsuke Yamane [a], Lisa Kitajima [b], Saeko Uchida [b], Akihiro Hamasaki [a], Eri Mukai [a,c], Kentaro Toyoda [a], Chizumi Yamada [a], Yuichiro Yamada [a,d], Yutaka Seino [a,e], Nobuya Inagaki [a,f,*]

[a] Department of Diabetes and Clinical Nutrition, Graduate School of Medicine, Kyoto University, Kyoto, Japan
[b] Molecular Function and Pharmacology Laboratories, Taisho Pharmaceutical Co., Ltd., Saitama, Japan
[c] Japan Association for the Advancement of Medical Equipment, Tokyo, Japan
[d] Department of Endocrinology and Diabetes and Geriatric Medicine, Akita University School of Medicine, Akita, Japan
[e] Kansai Electric Power Hospital, Osaka, Japan
[f] CREST of Japan Science and Technology Cooperation (JST), Kyoto, Japan

ARTICLE INFO

Article history:
Received 10 February 2009
Accepted 28 March 2009

Keywords:
Dipeptidyl peptidase-IV (DPP-IV)
DPP-IV inhibitor
Incretin
Glucagon-like peptide-1 (GLP-1)
Gastric inhibitory polypeptide (GIP)

ABSTRACT

Aim: Glucagon-like peptide-1 (GLP-1) and gastric inhibitory polypeptide (GIP) are major incretins associated with body weight regulation. Dipeptidyl peptidase-IV (DPP-IV) inhibitor increases plasma active GLP-1 and GIP. However, the magnitude of the effects of enhanced GLP-1 and GIP signaling by long-term DPP-IV inhibition on body weight and insulin secretion has not been determined. In this study, we compared the effects of long-term DPP-IV inhibition on body composition and insulin secretion of high fat diet (HFD)-fed wild-type (WT) and GLP-1R knockout (*GLP-1R*$^{-/-}$) mice.
Main methods: HFD-fed WT and *GLP-1R*$^{-/-}$ mice were treated with or without DPP-IV inhibitor by drinking water. Food and water intake and body weight were measured during 8 weeks of study. CT-based body composition analysis, Oral glucose tolerance test (OGTT), batch incubation study for insulin secretion and quantitative RT-PCR for expression of incretin receptors in isolated islets were performed at the end of study.
Key findings: DPP-IV inhibitor had no effect on food and water intake and body weight, but increased body fat mass in *GLP-1R*$^{-/-}$ mice. DPP-IV inhibitor-treated WT and *GLP-1R*$^{-/-}$ mice both showed increased insulin secretion in OGTT. In isolated islets of DPP-IV inhibitor-treated WT and *GLP-1R*$^{-/-}$ mice, glucose-induced insulin secretion was increased and insulin secretion in response to GLP-1 or GIP was preserved, without downregulation of incretin receptor expression.
Significance: Long-term DPP-IV inhibition may maintain body composition through counteracting effects of GLP-1 and GIP while improving glucose tolerance by increasing glucose-induced insulin secretion through the synergistic effects of GLP-1 and GIP.

Introduction

Oral glucose administration leads to much greater insulin release than the equivalent intravenous glucose challenge. Gut hormonal substances released in response to glucose include the incretins glucagon-like peptide-1 (GLP-1) and gastric inhibitory polypeptide /glucose-dependent insulinotropic peptide (GIP), which are responsible for ~50% of postprandial insulin release. GLP-1 and GIP potentiate glucose-induced insulin secretion from pancreatic β-cells by binding their respective receptors and subsequently increasing the intracellular cAMP concentration. In addition to their action on the enteroinsular axis, GLP-1 inhibits glucagon secretion (Komatsu et al. 1989), delays gastric emptying (Willms et al. 1996), decreases body weight through suppression of appetite (Turton et al. 1996), and suppresses β-cell apoptosis (Toyoda et al. 2008), while GIP enhances energy storage in adipocytes (Miyawaki et al. 2002) and calcium accumulation in bone (Tsukiyama et al. 2006). Thus, the incretins are associated with various systems of metabolic homeostasis, including that of both glucose and body weight.

However, the effects of GLP-1 and GIP are limited by their short half-life of a few minutes, which is primarily due to the action of dipeptidyl peptidase-IV (DPP-IV). DPP-IV is an enzyme distributed throughout the body including plasma and the endothelial lining of several organs, and cleaves two amino acids of biologically active peptides including GLP-1 and GIP by recognizing proline or alanine in the second N-terminal amino acid. The resulting N-terminal-truncated forms of GLP-1 and GIP are devoid of bioactivity. Since DPP-IV-deficient rodents show improved glucose tolerance and increased insulin secretion with elevated plasma active GLP-1 levels after oral glucose loading (Marguet et al. 2000; Nagakura et al. 2001), DPP-IV inhibitor and DPP-IV-resistant GLP-1

* Corresponding author. Department of Diabetes and Clinical Nutrition, Graduate School of Medicine, Kyoto University, 54 Shogoin Kawahara-cho, Sakyo-ku, Kyoto 606-8507, Japan. Tel.: +81 75 751 3560; fax: +81 75 751 4244.
E-mail address: inagki@metab.kuhp.kyoto-u.ac.jp (N. Inagaki).

0024-3205/$ – see front matter © 2009 Elsevier Inc. All rights reserved.
doi:10.1016/j.lfs.2009.03.022

receptor agonist are potential targets for the treatment of type 2 diabetes mellitus as a new class of antidiabetic agent. GLP-1 receptor agonist both increases insulin secretion and improves glucose tolerance and decreases body weight in rodents and humans (Szayna et al. 2000; Buse et al. 2004). DPP-IV inhibitor also increases insulin secretion and improves glucose tolerance, but its effect on body weight is controversial (Pospisilik et al. 2002; Lamont and Drucker 2008; Reimer et al. 2002; Ahrén et al. 2002). It is reported that DPP-IV inhibitor do not increase insulin secretion after glucose loading in GLP-1 receptor (GLP-1R)/GIP receptor (GIPR) double knockout (DIRKO) mice, indicating that both GLP-1 and GIP are critically involved in the insulinotropic action of long-term DPP-IV inhibition (Flock et al. 2007). However, the magnitude of the effects of enhanced GLP-1 and GIP signaling by long-term DPP-IV inhibition on body weight and insulin secretion has not been determined.

In the present study, we investigated the long-term effects of DPP-IV inhibition on body composition and insulin secretion using high fat diet (HFD)-fed wild-type (WT) and GLP-1R knockout (*GLP-1R*$^{-/-}$) mice.

Materials and methods

Animals

Mice (C57BL/6 background) were housed under a light/dark cycle of 12 h with free access to food and water. As ingestion of a meal rich in fat is a strong stimulus of incretin signaling (Harada et al. 2008), male WT and *GLP-1R*$^{-/-}$ mice were fed a high fat diet (45% fat, 20% protein and 35% carbohydrate by energy) from 7 weeks of age. Groups of treated HFD-fed WT and *GLP-1R*$^{-/-}$ mice received DPP-IV inhibitor in drinking water (0.5% W/V), while groups of untreated HFD-fed WT and *GLP-1R*$^{-/-}$ mice received drinking water without DPP-IV inhibitor. All the *GLP-1R*$^{-/-}$ mice were genotyped by Southern blot analysis. The DPP-IV inhibitor, provided by Taisho Pharmaceutical Co., Ltd., showed an inhibitory action on DPP-IV enzymatic activity against substrate H-Gly-Pro-7-amino-4-methyl coumarin (Gly-Pro-AMC) with IC_{50} (half maximal inhibitory concentration) of 0.0046 uM (Fukushima et al. 2008), while its IC_{50} on DPP-8 and DPP-9 were only 1.34 uM and 0.527 uM, respectively (unpublished data). Throughout the 8 weeks of study, water and food intake and body weight were measured once every 3 days. All mice care and procedures were approved by the Animal Care Committee of Kyoto University.

CT-based body composition analysis

The WT and *GLP-1R*$^{-/-}$ mice treated with or without DPP-IV inhibitor for 8 weeks were anesthetized and scanned along the body axis using LaTheta (LCT-100M) experimental animal CT system (Aloka, Tokyo, Japan). Contiguous 1-mm slice images of the whole abdominal cavity were used for quantitative assessment using LaTheta software (version 1.00). Weights of total fat mass, which comprises visceral fat mass and subcutaneous fat mass, and lean mass were quantitatively evaluated.

Oral glucose tolerance test (OGTT)

The WT and *GLP-1R*$^{-/-}$ mice treated with or without DPP-IV inhibitor for 8 weeks were fasted for 16 h and administered glucose (2 g/kg weight body) orally. Blood was collected from the orbital sinus of the mice at the indicated times (0, 15, 30, 60 and 120 min after glucose loading). Blood glucose levels were measured by the enzyme-electrode method. Plasma insulin levels were measured using an ELISA kit (Shibayagi, Gunma, Japan).

Measurement of plasma active GLP-1 levels and DPP-IV activity

For measurement of active GLP-1 levels, blood collected at 15 min after oral glucose loading was mixed with 2% EDTA· 4Na and 1% DPP-IV inhibitor (Linco Research, St Charles, MO). Active GLP-1 levels in plasma obtained by centrifugation (2000× g, 10 min, 4 °C) were measured using an active GLP-1 (7–36) ELISA kit (Linco Research).

Plasma DPP-IV activity was measured using a published method (Fukushima et al. 2008). In brief, 12.5 μl of plasma in duplicate was incubated with 37.5 μl of substrate cocktail (66.7 μM Gly-Pro-AMC, 25 mM HEPES, 140 mM NaCl, 26.6 mM $MgCl_2$, and 1% (w/v) BSA, pH 7.8) in the dark at room temperature for 5 min. The reaction was stopped by addition of 50 μl of 25% (v/v) acetic acid. Fluorescence was measured using a spectrofluorometer at excitation 360 nm/emission 465 nm. A standard curve was drawn using free AMC in standard buffer (25 mM HEPES, 140 mM NaCl, 20 mM $MgCl_2$, 1% (w/v) BSA, pH 7.8). DPP-IV activity (mU) is shown as the AMC (μM) generated in 1 ml plasma for 1 min of reaction time.

Measurement of insulin secretion in isolated islets

Islets were isolated from mice and preincubated at 37 °C for 30 min in 20 ml of Krebs-Ringer bicarbonate buffer (KRBB; 120 mM NaCl, 4.7 mM KCl, 1.2 mM $MgSO_4$, 1.2 mM KH_2PO_4, 2.4 mM $CaCl_2$, 20 mM $NaHCO_3$) supplemented with 10 mM HEPES and 0.2% (w/v) BSA and gassed with a mixture of 95% O_2 and 5% CO_2 (KRBB medium) containing 2.8 mM glucose. 10 size-matched islets collected in each tube were incubated at 37 °C for 30 min in 700 μl of KRBB medium containing 2.8 mM or 11.1 mM glucose with or without incretin peptides (100 nM human GLP-1 or 100 nM human GIP (Peptide Institute, Inc. Osaka, Japan)). Islets were then pelleted by centrifugation (9000× g, 2 min, 4 °C) and aliquots of the buffer were sampled. The amount of immunoreactive insulin was determined by radio-immunoassay (RIA). To determine insulin content, islets were homogenized in 400 μl acid-ethanol (37% HCl in 75% ethanol, 15:1000 (v/v)) and extracted at 4 °C overnight. The acidic extracts were dried by vacuum, reconstituted, and subjected to insulin measurement.

Measurement of mRNA expression of GLP-1R and GIPR in isolated islets

Measurement of mRNA expression of GLP-1R and GIPR was performed by quantitative RT-PCR as described previously (Harada et al. 2008). Briefly, total RNA was extracted from isolated islets with RNeasy mini kit (Qiagen, Valencia, CA) and treated with DNase (Qiagen). First strand cDNA was synthesized by SuperScript™ II Reverse Transcriptase system (Invitrogens, Grand Island, NY) according to manufacturer's instructions. SYBER Green PCR Master Mix (Applied Biosystems) was prepared for the PCR run. The PCR included 2 min at 50 °C and 10 min at 90 °C, followed by 50 cycles at 95 °C for 15 s and at 60 °C for 1 minute. The sequences of GLP-1R primers were 5′-CAACCGGACCTTTGATGACTA-3′ and 5′-GCTGTGCAGAACCGGTACAC-3′; the sequences of GIPR primers were 5′-CCTCCACTGGTCCCTACAC-3′ and 5′-GATAAACACCCTCCACCAGTAG-3′; the sequences of GAPDH primers were 5′-AAATGGTGAAGGTCGGTGTG-3′ and 5′-TCGTTGATGGCAACAATCTC-3′.

Statistical analyses

Data are expressed as means ± SE. Statistical analyses were performed by ANOVA and unpaired student's *t* test. *P* values<0.05 were considered significant.

Results

Body weight and body composition of DPP-IV inhibitor-treated HFD-fed mice

Water intake, food intake, and body weight of HFD-fed WT and *GLP-1R*$^{-/-}$ mice with or without DPP-IV inhibitor administration were measured. In WT mice, water and food intake in DPP-IV

inhibitor-treated and untreated mice were similar during the 8 weeks of the study (Fig. 1A). In *GLP-1R*$^{-/-}$ mice, water and food intake in DPP-IV inhibitor-treated and untreated mice also were similar (Fig. 1A). A significant difference in body weight between DPP-IV inhibitor-untreated WT and *GLP-1R*$^{-/-}$ mice appeared from the 36th day (30.9 ± 1.3 g vs. 27.0 ± 0.6 g, $P<0.05$) (Fig. 1B). Body weight of WT mice and *GLP-1R*$^{-/-}$ mice was unaffected by DPP-IV inhibitor treatment during the 8 weeks of the study. To measure the effect of DPP-IV inhibitor on body composition, CT-based analysis was performed (Fig. 1C). In WT mice, there was no significant difference in body fat ratio between DPP-IV inhibitor-treated and untreated mice. However, the body fat ratio of DPP-IV inhibitor-treated *GLP-1R*$^{-/-}$ mice was significantly increased compared with that of untreated *GLP-1R*$^{-/-}$ mice (44.13 ± 1.55 vs. 32.60 ± 3.50, $P<0.05$).

OGTT of DPP-IV inhibitor-treated mice

In OGTT, blood glucose levels at 30 and 60 min were significantly lower in DPP-IV inhibitor-treated WT and *GLP-1R*$^{-/-}$ mice compared to those in untreated WT and *GLP-1R*$^{-/-}$ mice, respectively (Fig. 2A). In WT mice, the plasma insulin level of DPP-IV inhibitor-treated mice was 2.3 times higher at 15 min than that of untreated control mice ($P<0.05$), while in *GLP-1R*$^{-/-}$ mice, the plasma insulin levels of DPP-IV inhibitor-treated mice were 1.6 and 1.4 times higher at 15 and 30 min than those of untreated control mice, respectively ($P<0.05$) (Fig. 2B). In addition, the plasma insulin level of DPP-IV inhibitor-treated WT mice was 1.6 times higher at 15 min compared with that of DPP-IV inhibitor-treated *GLP-1R*$^{-/-}$ mice ($P<0.05$) (Fig. 2B).

We also measured plasma DPP-IV activity and active GLP-1 levels in WT and *GLP-1R*$^{-/-}$ mice at 15 min by OGTT. 75–80% of plasma DPP-IV activity in both untreated WT and *GLP-1R*$^{-/-}$ mice was inhibited by DPP-IV inhibitor treatment (Fig. 2C). Plasma levels of active GLP-1 were significantly elevated in DPP-IV inhibitor-treated WT and *GLP-1R*$^{-/-}$ mice compared to those in the respective untreated mice (Fig. 2D).

Insulin secretion and incretin receptor expression of islets isolated from DPP-IV inhibitor-treated mice

To determine insulin secretion in response to glucose and GLP-1 and GIP, batch incubation experiments were performed using islets isolated from WT and *GLP-1R*$^{-/-}$ mice after 8 weeks of treatment (Fig. 3A). In islets of WT mice, insulin secretion in response to 2.8 mM glucose was similar in DPP-IV inhibitor-treated and untreated mice. However, insulin secretion in response to 11.1 mM glucose, 11.1 mM glucose with GLP-1, and 11.1 mM glucose with GIP was significantly higher in DPP-IV inhibitor-treated mice than those in untreated mice. In addition, both GLP-1 and GIP augmented insulin secretion in the presence of 11.1 mM glucose in both DPP-IV inhibitor-treated and untreated mice. In islets of *GLP-1R*$^{-/-}$ mice, as in those of WT mice, insulin secretion in response to 2.8 mM glucose was similar in DPP-IV inhibitor-treated and untreated mice, and insulin secretion in response to 11.1 mM glucose, 11.1 mM glucose with GLP-1, and 11.1 mM glucose with GIP was significantly higher in DPP-IV inhibitor-treated mice than those in untreated mice. However, in *GLP-1R*$^{-/-}$ mice, potentiation of insulin secretion by incretin in the presence of 11.1 mM glucose was observed only by GIP and not by GLP-1 in both DPP-IV inhibitor-treated and untreated mice. Insulin content was similar among all groups of mice (data not shown).

To determine the effect of DPP-IV inhibitor treatment on the mRNA expression of GLP-1R and GIPR in islets, we performed quantitative RT-PCR after 8 weeks of study (Fig. 3B). The mRNA expression levels of GLP-1R and GIPR in DPP-IV inhibitor-treated and untreated WT mice were similar, as were total mRNA expression levels of GIPR in DPP-IV inhibitor-treated and untreated *GLP-1R*$^{-/-}$ mice.

Discussion

In the present study, we evaluated body composition and glucose control in the absence of the GLP-1 signaling using *GLP-1R*$^{-/-}$ mice treated with DPP-IV inhibitor for 8 weeks to clarify GLP-1 and GIP action under long-term DPP-IV inhibition.

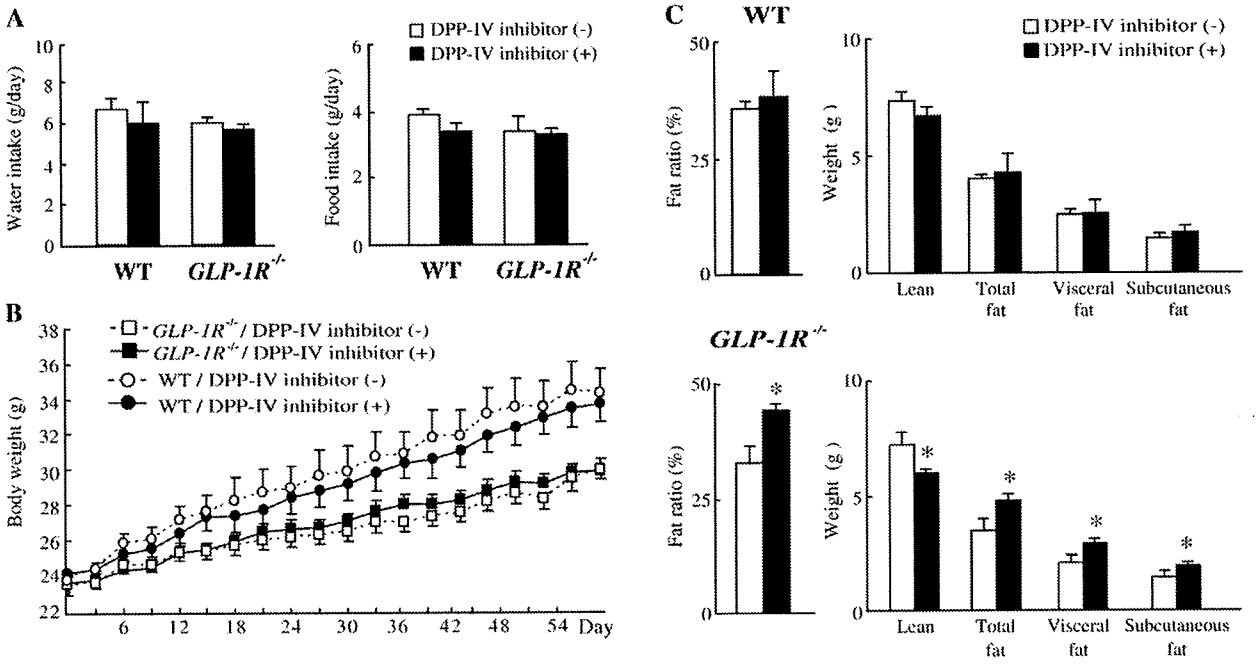

Fig. 1. Water and food intake, body weight and CT-based body composition analysis. (A) Water intake (left) and food intake (right) of WT and *GLP-1R*$^{-/-}$ mice treated with (filled) or without (open) DPP-IV inhibitor at the last week of study (average of 1 day). (B) Body weight change of WT (circle) and *GLP-1R*$^{-/-}$ (square) mice treated with (filled) or without (open) DPP-IV inhibitor. (C) CT-based body composition analysis of WT (upper) and *GLP-1R*$^{-/-}$ (lower) mice treated with (filled) or without (open) DPP-IV inhibitor. Fat ratio calculated as: total fat/(lean + total fat) × 100. Values are means ± SE. *$P<0.05$ vs. untreated mice ($n = 5$–6).

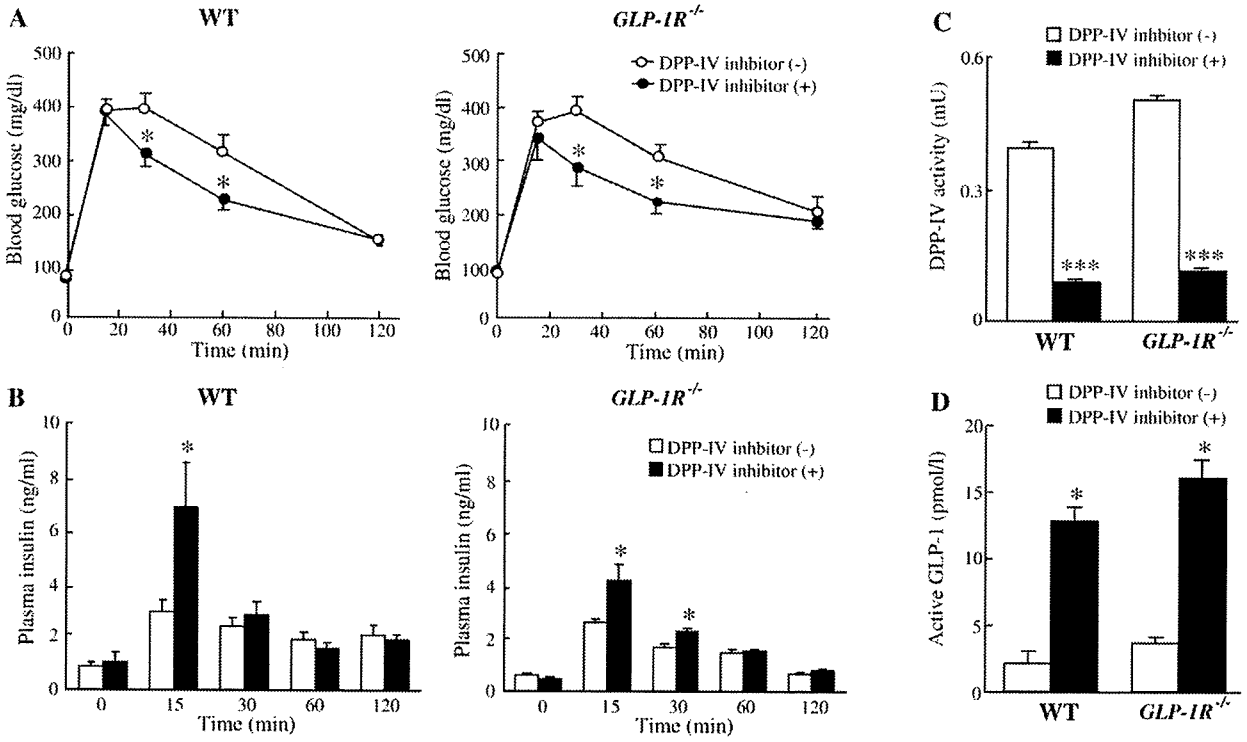

Fig. 2. OGTT. Blood glucose levels (A) and plasma insulin levels (B) of WT (left) and *GLP-1R*$^{-/-}$ (right) mice treated with (filled) or without (open) DPP-IV inhibitor after 8 weeks of study. Plasma DPP-IV activity (C) and plasma levels of active GLP-1 (D) at 15 min for WT and *GLP-1R*$^{-/-}$ mice treated with (filled) or without (open) DPP-IV inhibitor. Values are means ± SE. **P*<0.05, ****P*<0.001 vs. untreated mice (*n* = 5–6).

HFD-fed DPP-IV-deficient rodents exhibit reduced food intake and resistance to development of obesity with elevated active GLP-1 levels (Yasuda et al. 2002; Conarello et al. 2003), and DPP-IV inhibitor has been shown to reduce body weight in some previous studies using rodent models (Pospisilik et al. 2002; Lamont and Drucker 2008). In the present study, no alteration in body weight was found after 8 weeks of DPP-IV inhibitor treatment either in HFD-fed WT or *GLP-1R*$^{-/-}$ mice, although 75–80% of plasma DPP-IV activity was inhibited and plasma active GLP-1 levels were significantly elevated after oral glucose loading. However, CT-based body composition analysis revealed that DPP-IV inhibitor treatment increased body fat mass in *GLP-1R*$^{-/-}$ mice but not in WT mice. DPP-IV is well known to be involved in inactivation of both GLP-1 and GIP, and plasma active GIP levels are elevated by treatment of DPP-IV inhibitor (Deacon et al. 2001). The receptor for GIP, differently from that for GLP-1, is expressed in adipocytes, and GIP directly facilitates energy accumulation in adipose tissue (Miyawaki et al. 2002; Naitoh et al. 2008). Our results suggest that fat accumulation is potentiated by fat-augmenting factors including GIP in the absence of the GLP-1 signaling under long-term DPP-IV inhibition. Thus, the lack of change in body weight and fat mass in DPP-IV inhibitor-treated WT mice may be due to the counteracting effects of enhanced GLP-1 and GIP signaling. In addition, *GLP-1R*$^{-/-}$ mice showed less body weight gain compared to that of WT mice, consistent with the previous report on *GLP-1R*$^{-/-}$

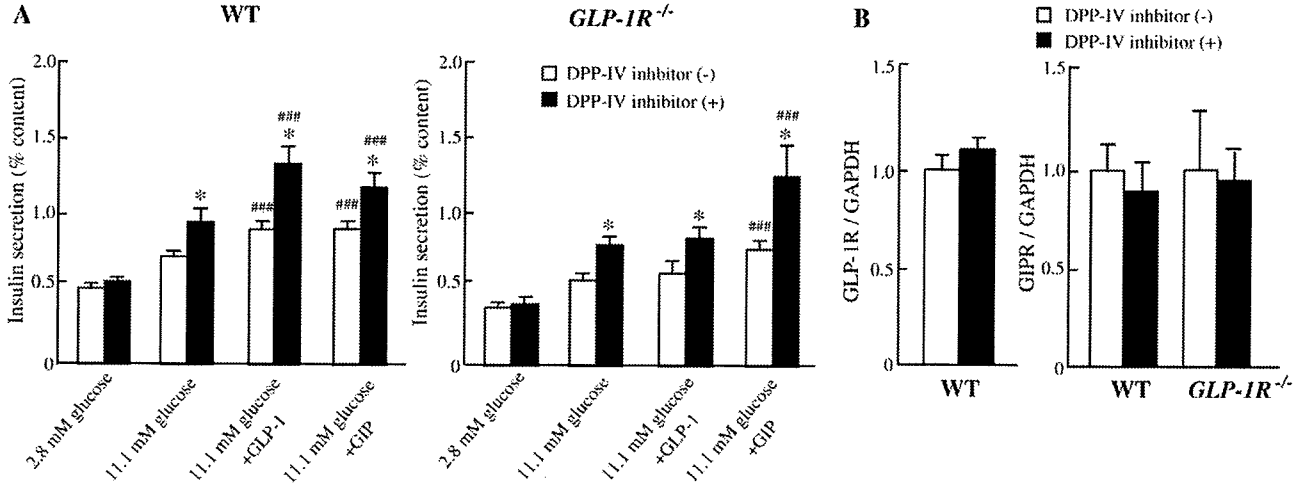

Fig. 3. Functional study of isolated islets. (A) Insulin secretion from islets isolated from WT (left) and *GLP-1R*$^{-/-}$ (right) mice treated with (filled) or without (open) DPP-IV inhibitor after 8 weeks of study. Values are means ± SE. **P*<0.05 vs. untreated mice. ###*P*<0.05 vs. 11.1 mM glucose. (B) The mRNA expression of GLP-1R and GIPR in islets isolated from WT and *GLP-1R*$^{-/-}$ mice treated with (filled) or without (open) DPP-IV inhibitor. GLP-1R and GIPR mRNA levels were corrected for GAPDH mRNA levels, respectively. Data of DPP-IV inhibitor-treated mice is shown relative to untreated mice. Values are means ± SE. (*n* = 5–8).

mice showing reduced body weight gain compared to that of WT mice, possibly due to enhanced locomotor activity and increased energy expenditure (Hansotia et al. 2007).

GLP-1 and GIP both are clearly involved in the effects of long-term DPP-IV inhibition on improved glucose tolerance, as DPP-IV inhibitor fails to increase insulin secretion and decrease plasma glucose after oral glucose loading in DIRKO mice (Flock et al. 2007). Our comparison in the present study of *GLP-1R*$^{-/-}$ mice and WT mice enables us to estimate the magnitude of the effects of enhanced GLP-1 and GIP by long-term DPP-IV inhibition on insulin secretion separately. Improved glucose tolerance and increased plasma insulin with elevated active GLP-1 levels were found in both DPP-IV inhibitor-treated WT and *GLP-1R*$^{-/-}$ mice by OGTT, indicating that GIP contributes to the insulinotropic effects of long-term DPP-IV inhibition in *GLP-1R*$^{-/-}$ mice. Moreover, blood insulin at 15 min in DPP-IV inhibitor-treated *GLP-1R*$^{-/-}$ mice was about half of that in DPP-IV inhibitor-treated WT mice. These results confirm that GLP-1 and GIP are important mediators of the insulinotropic effects of long-term DPP-IV inhibition. In addition, insulin secretion from islets in response to 11.1 mM glucose was increased in DPP-IV inhibitor-treated WT and *GLP-1R*$^{-/-}$ mice, indicating that glucose sensitivity of insulin secretion is augmented by long-term DPP-IV inhibitor administration unrelated to the GLP-1 signaling. However, the mechanism is not known. A recent report found that the glucose sensitivity of insulin secretion in isolated islets of mice improved after GLP-1 receptor agonist treatment due to augmented cAMP-induced activation of protein kinase A (PKA) through the GLP-1 receptor (Winzell and Ahrén 2008). It also was reported that activated PKA due to GLP-1 signaling increased expression of transcription factor pancreatic-duodenum homeobox-1 (PDX-1), translocation of PDX-1 from cytoplasm to nucleus, and phosphorylation of glucose transporter type 2 (GLUT2) in β-cells (Wang et al. 2001; Thorens et al. 1996). Thus, the increased glucose sensitivity of insulin secretion in islets unrelated to the GLP-1 signaling may be the result of augmented GIP signaling due long-term DPP-IV inhibition through similar mechanisms. Further study is required to clarify the augmentation of glucose sensitivity of islets after long-term DPP-IV inhibitor administration.

In addition to the plasma active incretin level, the expression of incretin receptors in islets also influences their insulinotropic effect (Lynn et al. 2001; Xu et al. 2007). Indeed, it has been reported that continuous GLP-1 stimulation results in desensitization of GLP-1R, which can subsequently reduce insulin secretion in response to GLP-1 in insulin-secreting cell lines (Widmann et al. 1996; Green et al. 2005). However, the expression of GLP-1R and GIPR in islets did not change in DPP-IV inhibitor-treated mice in the present study. Furthermore, insulin secretion in response to incretins was maintained in the islets of DPP-IV inhibitor-treated mice, demonstrating that sensitivity of the incretin receptors did not decrease even after 8 weeks of continuous incretin stimulation. These results suggest that the action of DPP-IV inhibitor in glucose control is preserved during long-term DPP-IV inhibitor administration.

Conclusion

Long-term DPP-IV inhibition does not alter body composition, possibly due to the counteracting effects of enhanced GLP-1 and GIP, but does improve glucose tolerance through the synergistic insulinotropic effects of enhanced GLP-1 and GIP, as well as by improved glucose responsiveness in pancreatic islets.

Acknowledgments

We thank Dr. Daniel. J. Drucker (Department of Medicine, The Banting and Best Diabetes Centre, Toronto General Hospital, University of Toronto, Toronto, Canada) for providing the *GLP-1R*$^{-/-}$ mice.

The funding of this study was supported by Scientific Research Grants from the Ministry of Education, Culture, Sports, Science, and Technology (Japan) and from the Ministry of Health, Labor, and Welfare (Japan).

References

Ahrén B, Simonsson E, Larsson H, Landin-Olsson M, Torgeirsson H, Jansson PA, Sandqvist M, Båvenholm P, Efendic S, Eriksson JW, Dickinson S, Holmes D. Inhibition of dipeptidyl peptidase IV improves metabolic control over a 4-week study period in type 2 diabetes. Diabetes Care 25 (5), 869–875, 2002.

Buse JB, Henry RR, Han J, Kim DD, Fineman MS, Baron AD. Exenatide-113 Clinical Study Group. Effects of Exenatide (Exendin-4) on glycemic control over 30 weeks in sulfonylurea-treated patients with type 2 diabetes. Diabetes Care 27 (11), 2628–2635, 2004.

Conarello SL, Li Z, Ronan J, Roy RS, Zhu L, Jiang G, Liu F, Woods J, Zycband E, Moller DE, Thornberry NA, Zhang BB. Mice lacking dipeptidyl peptidase IV are protected against obesity and insulin resistance. Proceedings of the National Academy of Sciences of the United States of America 100 (11), 6825–6830, 2003.

Deacon CF, Danielsen P, Klarskov L, Olesen M, Holst JJ. Dipeptidyl peptidase IV inhibition reduces the degradation and clearance of GIP and potentiates its insulinotropic and antihyperglycemic effects in anesthetized pigs. Diabetes 50 (7), 1588–1597, 2001.

Flock G, Baggio LL, Longuet C, Drucker DJ. Incretin receptors for glucagon-like peptide 1 and glucose-dependent insulinotropic polypeptide are essential for the sustained metabolic actions of Vildagliptin in mice. Diabetes 56 (12), 3006–3013, 2007.

Fukushima H, Hiratate A, Takahashi M, Mikami A, Saito-Hori M, Munetomo E, Kitano K, Chonan S, Saito H, Suzuki A, Takaoka Y, Yamamoto K. Synthesis and structure–activity relationships of potent 4-fluoro-2-cyanopyrrolidine dipeptidyl peptidase IV inhibitors. Bioorganic & Medicinal Chemistry 16 (7), 4093–4106, 2008.

Green BD, Liu HK, McCluskey JT, Duffy NA, O'Harte FP, McClenaghan NH, Flatt PR. Function of a long-term, GLP-1-treated, insulin-secreting cell line is improved by preventing DPP IV-mediated degradation of GLP-1. Diabetes, Obesity & Metabolism 7 (5), 563–569, 2005.

Hansotia T, Maida A, Flock G, Yamada Y, Tsukiyama K, Seino Y, Drucker DJ. Extrapancreatic incretin receptors modulate glucose homeostasis, body weight, and energy expenditure. The Journal of Clinical Investigation 117 (1), 143–152, 2007.

Harada N, Yamada Y, Tsukiyama K, Yamada C, Nakamura Y, Mukai E, Hamasaki A, Liu X, Toyoda K, Seino Y, Inagaki N. A novel gastric inhibitory polypeptide (GIP) receptor splice variant influences GIP sensitivity of pancreatic {beta}-cells in obese mice. American Journal of Physiology. Endocrinology and Metabolism 294 (1), E61–E68, 2008.

Komatsu R, Matsuyama T, Namba M, Watanabe N, Itoh H, Kono N, Tarui S. Glucagonostatic and insulinotropic action of glucagon-like peptide-1-(7-36) amide. Diabetes 38 (7), 902–905, 1989.

Lamont BJ, Drucker DJ. Differential antidiabetic efficacy of incretin agonists versus DPP-4 inhibition in high fat-fed mice. Diabetes 57 (1), 190–198, 2008.

Lynn FC, Pamir N, Ng EH, McIntosh CH, Kieffer TJ, Pederson RA. Defective glucose-dependent insulinotropic polypeptide receptor expression in diabetic fatty zucker rats. Diabetes 50 (5), 1004–1011, 2001.

Marguet D, Baggio L, Kobayashi T, Bernard AM, Pierres M, Nielsen PF, Ribel U, Watanabe T, Drucker DJ, Wagtmann N. Enhanced insulin secretion and improved glucose tolerance in mice lacking CD26. Proceedings of the National Academy of Sciences of the United States of America 97 (12), 6874–6879, 2000.

Miyawaki K, Yamada Y, Ban N, Ihara Y, Tsukiyama K, Zhou H, Fujimoto S, Oku A, Tsuda K, Toyokuni S, Hiai H, Mizunoya W, Fushiki T, Holst JJ, Makino M, Tashita A, Kobara Y, Tsubamoto Y, Jinnouchi T, Jomori T, Seino Y. Inhibition of gastric inhibitory polypeptide signaling prevents obesity. Nature Medicine 8 (7), 738–742, 2002.

Nagakura T, Yasuda N, Yamazaki K, Ikuta H, Yoshikawa S, Asano O, Tanaka I. Improved glucose tolerance via enhanced glucose-dependent insulin secretion in dipeptidyl peptidase IV-deficient Fischer rats. Biochemical and Biophysical Research Communications 284 (2), 501–506, 2001.

Naitoh R, Miyawaki K, Harada N, Mizunoya W, Toyoda K, Fushiki T, Yamada Y, Seino Y, Inagaki N. Inhibition of GIP signaling modulates adiponectin levels under high-fat diet in mice. Biochemical and Biophysical Research Communications 376 (1), 21–25, 2008.

Pospisilik JA, Stafford SG, Demuth HU, Brownsey R, Parkhouse W, Finegood DT, McIntosh CH, Pederson RA. Long-term treatment with the dipeptidyl peptidase IV inhibitor P32/98 causes sustained improvements in glucose tolerance, insulin sensitivity, hyperinsulinemia, and β-cell glucose responsiveness in VDF (fa/fa) zucker rats. Diabetes 51 (4), 943–950, 2002.

Reimer MK, Holst JJ, Ahrén B. Long-term inhibition of dipeptidyl peptidase IV improves glucose tolerance and preserves islet function in mice. European Journal of Endocrinology/European Federation of Endocrine Societies 146 (5), 717–727, 2002.

Szayna M, Doyle ME, Betkey JA, Holloway HW, Spencer RG, Greig NH, Egan JM. Exendin-4 decelerates food intake, weight gain, and fat deposition in Zucker rats. Endocrinology 141 (6), 1936–1941, 2000.

Thorens B, Dériaz N, Bosco D, DeVos A, Pipeleers D, Schuit F, Meda P, Porret A. Protein kinase A-dependent phosphorylation of GLUT2 in pancreatic beta cells. The Journal of Biological Chemistry 271 (14), 8075–8081, 1996.

Toyoda K, Okitsu T, Yamane S, Uonaga T, Liu X, Harada N, Uemoto S, Seino Y, Inagaki N. GLP-1 receptor signaling protects pancreatic beta cells in intraportal islet transplant by inhibiting apoptosis. Biochemical and Biophysical Research Communications 367 (4), 793–798, 2008.

Tsukiyama K, Yamada Y, Yamada C, Harada N, Kawasaki Y, Ogura M, Bessho K, Li M, Amizuka N, Sato M, Udagawa N, Takahashi N, Tanaka K, Oiso Y, Seino Y. Gastric

inhibitory polypeptide as an endogenous factor promoting new bone formation after food ingestion. Molecular Endocrinology 20 (7), 1644–1651, 2006.
Turton MD, O'Shea D, Gunn I, Beak SA, Edwards CM, Meeran K, Choi SJ, Taylor GM, Heath MM, Lambert PD, Wilding JP, Smith DM, Ghatei MA, Herbert J, Bloom SR. A role for glucagon-like peptide-1 in the central regulation of feeding. Nature 379 (6560), 69–72, 1996.
Wang X, Zhou J, Doyle ME, Egan JM. Glucagon-like peptide-1 causes pancreatic duodenal homeobox-1 protein translocation from the cytoplasm to the nucleus of pancreatic beta-cells by a cyclic adenosine monophosphate/protein kinase A-dependent mechanism. Endocrinology 142 (5), 1820–1827, 2001.
Widmann C, Dolci W, Thorens B. Desensitization and phosphorylation of the glucagon-like peptide-1 (GLP-1) receptor by GLP-1 and 4-Phorbol 12-Myristate 13-Acetate. Molecular Endocrinology 10 (1), 62–75, 1996.
Willms B, Werner J, Holst JJ, Orskov C, Creutzfeldt W, Nauck MA. Gastric emptying, glucose responses, and insulin secretion after a liquid test meal: Effects of exogenous glucagon-like peptide-1 (GLP-1)-(7–36) amide in type 2 (noninsulin-dependent) diabetic patients. The Journal of Clinical Endocrinology and Metabolism 81 (1), 327–332, 1996.
Winzell MS, Ahrén B. Durable islet effects on insulin secretion and protein kinase A expression following exendin-4 treatment of high-fat diet-fed mice. Journal of Molecular Endocrinology 40 (2), 93–100, 2008.
Xu G, Kaneto H, Laybutt DR, Duvivier-Kali VF, Trivedi N, Suzuma K, King GL, Weir GC, Bonner-Weir S. Downregulation of GLP-1 and GIP receptor expression by hyperglycemia: Possible contribution to impaired incretin effects in diabetes. Diabetes 56 (6), 1551–1558, 2007.
Yasuda N, Nagakura T, Yamazaki K, Inoue T, Tanaka I. Improvement of high fat-diet-induced insulin resistance in dipeptidyl peptidase IV-deficient Fischer rats. Life Sciences 71 (2), 227–238, 2002.

THE JOURNAL OF BIOLOGICAL CHEMISTRY VOL. 285, NO. 9, pp. 6693–6705, February 26, 2010

Spontaneous Development of Endoplasmic Reticulum Stress That Can Lead to Diabetes Mellitus Is Associated with Higher Calcium-independent Phospholipase A_2 Expression

*A ROLE FOR REGULATION BY SREBP-1**

Received for publication, November 11, 2009, and in revised form, December 18, 2009 Published, JBC Papers in Press, December 23, 2009, DOI 10.1074/jbc.M109.084293

Xiaoyong Lei[‡], Sheng Zhang[‡], Suzanne E. Barbour[§], Alan Bohrer[‡], Eric L. Ford[‡], Akio Koizumi[¶], Feroz R. Papa[‖], and Sasanka Ramanadham[‡1]

From the [‡]Department of Medicine, Mass Spectrometry Resource, and Division of Endocrinology, Metabolism, and Lipid Research, Washington University School of Medicine, St. Louis, Missouri 63110, the [§]Department of Biochemistry and Molecular Biology, Virginia Commonwealth University School of Medicine, Richmond, Virginia 23298, the [¶]Department of Health and Environmental Sciences, Kyoto Graduate School of Medicine, Kyoto 606-8501, Japan, and the [‖]California Institute for Quantitative Biosciences, University of California, San Francisco, California 94143

Our recent studies indicate that endoplasmic reticulum (ER) stress causes INS-1 cell apoptosis by a Ca^{2+}-independent phospholipase A_2 (iPLA$_2\beta$)-mediated mechanism that promotes ceramide generation via sphingomyelin hydrolysis and subsequent activation of the intrinsic pathway. To elucidate the association between iPLA$_2\beta$ and ER stress, we compared β-cell lines generated from wild type (WT) and Akita mice. The Akita mouse is a spontaneous model of ER stress that develops hyperglycemia/diabetes due to ER stress-induced β-cell apoptosis. Consistent with a predisposition to developing ER stress, basal phosphorylated PERK and activated caspase-3 are higher in the Akita cells than WT cells. Interestingly, basal iPLA$_2\beta$, mature SREBP-1 (mSREBP-1), phosphorylated Akt, and neutral sphingomyelinase (NSMase) are higher, relative abundances of sphingomyelins are lower, and mitochondrial membrane potential ($\Delta\Psi$) is compromised in Akita cells, in comparison with WT cells. Exposure to thapsigargin accelerates $\Delta\Psi$ loss and apoptosis of Akita cells and is associated with increases in iPLA$_2\beta$, mSREBP-1, and NSMase in both WT and Akita cells. Transfection of Akita cells with iPLA$_2\beta$ small interfering RNA, however, suppresses NSMase message, $\Delta\Psi$ loss, and apoptosis. The iPLA$_2\beta$ gene contains a sterol-regulatory element, and transfection with a dominant negative SREBP-1 reduces basal mSREBP-1 and iPLA$_2\beta$ in the Akita cells and suppresses increases in mSREBP-1 and iPLA$_2\beta$ due to thapsigargin. These findings suggest that ER stress leads to generation of mSREBP-1, which can bind to the sterol-regulatory element in the iPLA$_2\beta$ gene to promote its transcription. Consistent with this, SREBP-1, iPLA$_2\beta$, and NSMase messages in Akita mouse islets are higher than in WT islets.

β-Cell loss due to apoptosis contributes to the progression and development of Type 1 or Type 2 diabetes mellitus (T1DM[2] or T2DM, respectively). This is supported by autopsy studies that reveal reduced β-cell mass in obese T2DM subjects in comparison with obese non-diabetic subjects (1, 2) and reveal that the loss in β-cell function in non-obese T2DM is associated with decreases in β-cell mass (3, 4). Other evidence suggests that cytokines cause β-cell apoptosis during the development of autoimmune T1DM (5–8). It is therefore important to understand the mechanisms underlying β-cell apoptosis if this process is to be prevented or delayed.

β-Cell mass is regulated by a balance between β-cell replication/neogenesis and β-cell death resulting from apoptosis (9, 10). Findings in rodent models of T2DM (10, 11) and in human T2DM (3, 4) indicate that the decrease in β-cell mass in T2DM is not attributable to reduced β-cell proliferation or neogenesis but to increased β-cell apoptosis (12). In addition to the intrinsic and extrinsic apoptotic pathways, apoptosis due to prolonged endoplasmic reticulum (ER) stress (12, 13) has been reported in various diseases, including Alzheimer and Parkinson diseases (14).

Evidence from the Akita (15, 16) and NOD.k iHEL (17) mouse models suggests that ER stress can also lead to the development of diabetes mellitus as a consequence of β-cell apoptosis. Further, mutations in genes encoding the ER stress-transducing enzyme pancreatic ER kinase (PERK) (18) and the ER-resident protein involved in degradation of malfolded ER proteins have been clinically linked to diminished β-cell health (19, 20). Other reports suggest that ER stress may also play a

* This work was supported, in whole or in part, by National Institutes of Health Grants R01-DK69455, P41-RR00954, P60-DK20579, P30-DK56341, and DK065671. This work was also supported by a grant from the American Diabetes Association (to S. R.) and National Science Foundation Grant NSF-MCB-0544068 (to S. E. B.).

[1] To whom correspondence should be addressed: Dept. of Medicine, Washington University School of Medicine, Campus Box 8127, 660 S. Euclid Ave., St. Louis, MO 63110. Tel.: 314-362-8194; Fax: 314-362-7641; E-mail: sramanad@dom.wustl.edu.

[2] The abbreviations used are: T1DM, Type 1 diabetes mellitus; T2DM, Type 2 diabetes mellitus; AK, Akita; pAkt, phosphorylated Akt; PERK, pancreatic ER kinase; pPERK, phosphorylated PERK; BEL, bromoenol lactone suicide inhibitor of iPLA$_2\beta$; DN, dominant negative; ER, endoplasmic reticulum; ESI/MS/MS, electrospray ionization/tandem mass spectrometry; GPC, glycerophosphocholine; iPLA$_2\beta$, β-isoform of group VIA Ca^{2+}-independent phospholipase A_2; NSMase, neutral sphingomyelinase; PBS, phosphate-buffered saline; PLA$_2$, phospholipase A_2; mSREBP-1, mature (or processed) SREBP-1; TUNEL, terminal deoxynucleotidyl transferase-mediated (fluorescein) dUTP nick end labeling; WT, wild type; siRNA, small interfering RNA; DAPI, 4′,6-diamidino-2-phenylindole; qRT-PCR, quantitative reverse transcription-PCR; SRE, sterol-regulatory element; DiOC$_6$(3), 3,3′-dihexyloxacarbocyanine iodide.

prominent role in the autoimmune destruction of β-cells during the development of T1DM (6, 21, 22). Because the secretory function of β-cells endows them with a highly developed ER and the β-cell is one of the cells most sensitive to nitric oxide (23), it is not unexpected that β-cells exhibit a heightened susceptibility to autoimmune-mediated ER stress (24, 25). In support of this, Wolfram syndrome, which is associated with juvenile onset diabetes mellitus, is recognized to be a consequence of chronic ER stress in pancreatic β-cells (21, 26).

In view of the evidence suggesting that ER stress-induced β-cell apoptosis may be a factor in the development of diabetes mellitus, it was of interest to elucidate the mechanisms involved. Recent work from our laboratory led to the identification of a Ca^{2+}-independent phospholipase A_2 (iPLA$_2\beta$) as a key participant in ER stress-mediated apoptosis of INS-1 insulinoma cells. The iPLA$_2\beta$, classified as a Group VIA isoform of iPLA$_2$, is a member of a large family of PLA$_2$s (27) that is cytosolic and does not require Ca^{2+} for activity (28–30). It is activated by ATP, is inhibited by the bromoenol lactone suicide substrate (BEL) inhibitor of iPLA$_2\beta$ (31), and is recognized to have a role in signal transduction (28, 31–39). We found that induction of ER stress with the sarcoendoplasmic reticulum Ca^{2+}-ATPase inhibitor thapsigargin causes INS-1 cell apoptosis that is amplified by overexpression of iPLA$_2\beta$ and is inhibited by BEL (40).

Further work indicated that ER stress activates iPLA$_2\beta$ in INS-1 cells, leading to neutral sphingomyelinase (NSMase) induction and generation of ceramides via hydrolysis of sphingomyelins (41). Subsequently, the ceramides trigger mitochondrial apoptotic processes and cell death ensues. Consistent with this proposed mechanism, inhibition of iPLA$_2\beta$ or NSMase suppresses sphingomyelin hydrolysis and ceramide generation, mitochondrial abnormalities, and apoptosis (42).

Although a link between iPLA$_2\beta$ and ER stress-induced apoptotic pathway was gleaned from the above observations, it was derived from studies in which a chemical agent was used to induce ER stress and iPLA$_2\beta$ expression levels were genetically manipulated in an insulinoma cell line. Of importance was to determine whether a similar link existed under conditions where ER stress developed in the β-cell in the absence of chemical intervention. Here, we present studies in a β-cell line established from Akita mice (43), which contain a spontaneous mutation of the insulin 2 gene (*Ins2*) (C96Y) that results in misfolding insulin in the ER leading to development of hyperglycemia/diabetes due to ER stress-induced β-cell apoptosis (44, 45). Our findings reveal for the first time that predisposition to ER stress is associated with increased expression of iPLA$_2\beta$ and that its expression is modulated by activation of SREBP-1 (sterol-regulatory element-binding protein-1). We also present the first evidence in Akita mouse islet β-cells that substantiates these findings.

EXPERIMENTAL PROCEDURES

Materials—The sources for the material used were as follows: 16:0/[^{14}C]18:2-GPC (55 mCi/mmol), rainbow molecular mass standards, and ECL reagent (Amersham Biosciences); low melting agarose (Applied Biosystems Inc., Foster City, CA); Coomassie reagent, SDS-PAGE supplies, and Triton X-100 (Bio-Rad); mitochondrial membrane potential detection kit (Cell Tech. Inc., Mountain View, CA); paraformaldehyde (Electron Microscopy Sciences, Ft. Washington, PA); xylene (Fisher); secondary antibody goat anti-rabbit IgG Alexa Fluor 594 (Invitrogen); secondary antibody Cy3-affinipure bovine anti-goat IgG(H + L) (Jackson ImmunoResearch Laboratories Inc., West Grove, PA); DiOC$_6$(3) and Hoechst dye and Slow Fade® light antifade kit (Molecular Probes, Inc., Eugene, OR); peroxidase-conjugated goat anti-rabbit IgG antibody, TUNEL kit (Roche Applied Science); Lipofectamine 2000 (Invitrogen); siRNA kit (Qiagen, Valencia, CA); primary antibodies (Santa Cruz Biotechnology, Inc., Santa Cruz, CA); agarose, collagenase, protease inhibitor mixture, thapsigargin, common reagents, and salts (Sigma); tissue marking dye (Triangle Biomedical Sciences Inc. (Durham, NC) and Vector Laboratories, Inc. (Burlingame, CA).

Cell Culture and Treatment—The Akita and wild type (WT) cells were generated as follows. A transgenic mouse line that harbored the modified human insulin promoter connected to the SV40 T antigen coding region on C57BL/6 mice (IT3 line) was kindly provided by Dr. Jun-Ichi Miyazaki (46). Male offspring were mated with female Akita mice (*Ins2*$^{+/AK}$) (45) on a C57BL/6 background. Insulinomas that developed in the pancreas of the progeny were removed and cultured in Dulbecco's modified Eagle's medium containing high glucose and 15% fetal bovine serum (43). Pancreatic β-cell lines were established from the cells grown as monolayers on culture dishes. Several cell lines were obtained for *Ins2*$^{+/AK}$ and for wild type *Ins2*$^{+/+}$.

The cells were cultured in Dulbecco's modified Eagle's medium (containing 10 μl of β-mercaptoethanol/200 ml) as described (43). The medium was exchanged every 2 days, and the cells were split, as required, once a week. Cells (~25–30 passages) were grown to 80% confluence in cell culture dishes and harvested following treatment with vehicle (DMSO, 0.50 μl/ml) or thapsigargin (0.5 μM). The cells were harvested at various times (2–16 h) and prepared for various analyses described below. All incubations were done at 37 °C under an atmosphere of 95% air, 5% CO_2.

In Situ Detection of DNA Cleavage by TUNEL and DAPI Staining—Cells were harvested and washed twice with ice-cold PBS and then immobilized on slides by cytospin (40) and fixed with 4% paraformaldehyde (in PBS, pH 7.4, 1 h, room temperature). The cells were then processed for TUNEL staining analyses as described (42). Incidence of apoptosis was assessed under a fluorescence microscope (Nikon Eclipse TE300) using a fluorescein isothiocyanate filter. Cells with TUNEL-positive nuclei were considered apoptotic. DAPI staining was used to determine the total number of cells in a field. A minimum of three fields per slide was used to calculate the percentage of apoptotic cells.

Assessment of Mitochondrial Membrane Potential (ΔΨ)—Loss of ΔΨ is an important step in the induction of cellular apoptosis (47). Akita and WT cell ΔΨ was initially measured using a commercial kit by flow cytometry (BD Biosciences) as described (42). Fluorescence in cells was monitored at an excitation wavelength of 488 nm. Although these analyses yield quantitative results, they were hampered by the tendency of these cells to clump together, causing the fluorescence peaks to

be broad. To address this issue, a second method to monitor $\Delta\Psi$ was established. Cells were plated in a 6-well plate with the coverslips and cultured up to semiconfluence. After washing with PBS twice at room temperature, the coverslips were incubated with $DiOC_6(3)$ solution (175 nM) for 15 min under an atmosphere of 5% CO_2, 95% air (37 °C). The Hoechst reagent (5 μg/ml) was then added to stain the nucleus. After 20 min, the coverslips were rinsed with PBS, mounted on slides, and the cells were immediately examined using a confocal laser-scanning microscope (Zeiss) with a 488-nm argon laser and a 405-nm diode laser.

Immunoblotting Analyses—Cells were harvested and sonicated, and an aliquot (30 μg) of lysate protein was analyzed by SDS-PAGE (8 or 15%), transferred onto Immobilon-P polyvinylidene difluoride membranes, and processed for immunoblotting analyses as described (40). The targeted factors and the primary antibody concentrations were as follows: phosphorylated PERK (pPERK) (1:1000), iPLA$_2$β (T-14) (1:500), caspase-3 (1:1000), SREBP-1 (1:1000), pAkt (1:1000), and tubulin (1:2000). The secondary antibody concentration was 1:10,000. Immunoreactive bands were visualized by ECL.

Assay for iPLA$_2$β Activity—Cytosol fraction was prepared from Akita and WT cells and harvested, and protein concentration was determined using Coomassie reagent. Ca^{2+}-independent PLA_2 catalytic activity in an aliquot of cytosolic protein (30 μg) was assayed under zero Ca^{2+} conditions (no added Ca^{2+} plus 10 mM EGTA) in the presence of 16:0/[^{14}C]18:2-GPC (5 μM) as the substrate, and specific enzymatic activity was quantitated as described (40). To verify that the phospholipase activity is manifested by iPLA$_2$β, activity was also assayed in the presence of ATP (10 mM) or BEL (1 μM).

Sphingomyelin Analyses by ESI/MS/MS—Sphingomyelins are formed by reaction of a ceramide with CDP-choline, and similar to GPC lipids, they contain a phosphocholine as the polar headgroup. This feature of sphingomyelins facilitates identification of sphingomyelin molecular species by constant neutral loss scanning of trimethylamine ($[M + H]^+ - N(CH_3)_3$) or constant neutral loss of 59 as described (41). The prominent ions in the total ion current spectrum are those of the even mass PC molecular species, and these mask the odd mass sphingomyelin signals (41). Constant neutral loss of 59, however, facilitates emergence of signals for sphingomyelin species at odd *m/z* values, reflecting loss of nitrogen. Lipid extracts were prepared as above in the presence of a 14:0/14:0-GPC (*m/z* 684, 8 μg) internal standard, which is not an endogenous component of β-cell lipids, and analyzed by ESI/MS/MS. Sphingomyelins content in the samples was determined based on standard curves generated using commercially available brain and egg sphingomyelins with a known percentage of each fatty acid constituent and 14:0/14:0-GPC (*m/z* 684, 8 μg) as an internal standard as described (41). Total (pmol) sphingomyelin species in each fraction was determined and normalized to total phosphate (μmol of PO_4).

Transient Transfection of Dominant Negative (DN) SREBP-1—A DN SREBP-1 vector (Addgene plasmid 8885) was obtained from Addgene (Cambridge, MA). The plasmid developed by Kim and Spiegelman (49) expresses truncated ADD1 with a tyrosine to alanine mutation at amino acid 320. WT and Akita cells were cultured as described above and transfected 1 day before 90–95% confluence using Lipofectamine 2000 (Invitrogen). Briefly, DN SREBP-1 was diluted in 50 μl of Opti-MEM I reduced serum medium and mixed gently. After a 5-min incubation, DN SREBP-1 was mixed with diluted Lipofectamine 2000 (total volume, 100 μl). The mixture was incubated for 20 min at room temperature and used to transfect WT and Akita cells cultured in a 6-well plate. The cells were incubated at 37 °C under an atmosphere of 95% air, 5% CO_2 for 48 h prior to experimentation.

Suppression of iPLA$_2$β Expression—To knock down iPLA$_2$β, wild type and Akita cells were transfected with iPLA$_2$β siRNA according to the manufacturer's instructions (Qiagen, Valencia, CA). Cells were seeded in wells with culture medium containing serum and antibiotics and allowed to reach 50–80% confluence. The cells were then transfected with either control siRNA (*si** in Fig. 7) or iPLA$_2$β siRNA (*si* in Fig. 7). The siRNAs were prepared in dilution buffer and mixed gently with RNAiFect transfection reagent. The mixture was then incubated at room temperature for 10–15 min to allow formation of transfection complexes. The complexes were then gently added to the cells. The cells were cultured with the transfection complexes at 37 °C under an atmosphere of 95% air, 5% CO_2 for 72 h prior to experimentation.

Islet Isolation—Male mice (4–5 weeks of age) were anesthetized with ketamine/xlyazine mixture (0.75 μl/g body weight) prior to euthanization by cervical dislocation. The abdomen was isolated, and pancreata were isolated as described (50). The common bile duct was clamped at the duodenum-bile duct junction, and collagenase/Krebs-Ringer buffer (5 ml) was injected into the pancreas via the duct. Once the pancreas was completely distended, it was removed and placed in a scintillation vial with collagenase/Krebs-Ringer buffer (2.5 ml) and incubated in a 37 °C water bath for 13 min. The vial was then vigorously shaken for 90 s, followed by washing (three times) of the pancreas with Krebs-Ringer buffer containing 1 mM $CaCl_2$ (50 ml). The pancreas was then resuspended in incomplete RPMI 1640 (without FBS or penicillin/streptomycin, 25 ml) and poured through a 70-μm cell strainer into a Petri dish. The cells were washed further with incomplete RPMI 1640 (75 ml). The cell strainer was then inverted and rinsed with complete RPMI 1640 (10% fetal bovine serum, 2× penicillin/streptomycin, 25 ml) to collect the remaining islets in solution. The islets were then hand-picked under a microscope, counted, and incubated overnight in media under an atmosphere of 5% CO_2, 95% and 37 °C. Typical islet yields ranged from 25 to 50 from the Akita mice and 150 from WT mice. The islets were used to prepare total RNA for message and for immunostaining analyses, as described below.

Quantitative Reverse Transcription-PCR (qRT-PCR)—Total RNA was prepared from cells and islets cells using the RNeasy kit (Qiagen Inc.) as described (41, 42). cDNA was then generated using the SuperScriptII kit (Invitrogen) and heat-inactivated (70 °C for 15 min). PCR amplifications were performed using the SYBR Green PCR kit in an ABI 7000 detection system (Applied Biosystems). The primers were designed based on known mouse sequences for iPLA$_2$β, SREBP-1, NSMase, and control 18 S provided in the GenBank™ data base with identi-

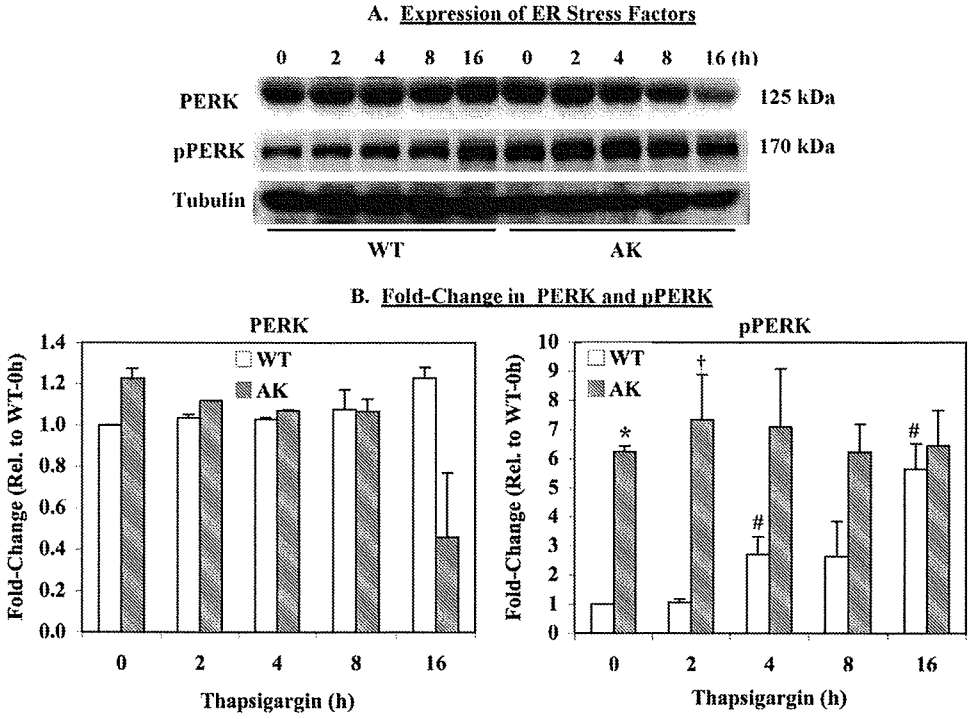

FIGURE 1. **Basal expression of ER stress factors and apoptotic factors.** WT and AK β-cells were harvested at various times after exposure to thapsigargin (0.50 μM), and 30 μg of lysate protein was processed for immunoblotting analyses for PERK and pPERK. Tubulin was used as a loading control. These analyses were done three separate times. *A*, immunoblot. A representative blot for PERK and pPERK is presented. *B*, densitometry. The ratios of PERK- and pPERK-immunoreactive bands to the corresponding tubulin band were determined, and means ± S.E. of -fold change relative to WT at 0 h are presented. * and †, significantly different from corresponding WT, $p < 0.001$ and $p < 0.05$, respectively. #, significantly different from WT at 0 h, $p < 0.05$.

fication numbers 53357, 20787, 20598, and 19791, respectively. The sense/antisense primer sets were as follows: iPLA$_2\beta$, gcccctggccattctacacagta/cacctcatccttcatacggaagt; SREBP-1, ccagaggtgagcctgacaa/agcctctgcaatttccagatct; NSMase, ctgagtacagccgacagaagga/gggccagttcccaagctt; 18 S, gccgctagaggtgaaattcttg/cattcttggcaaatgctttcg.

Immunostaining—Islets were fixed in 10% formalin and 5 μl of tissue marking dye, followed by the addition of 150 μl of low melting agarose. The mixture was spun down quickly to settle the islets at one surface of the agarose, which was then allowed to solidify. The islet-containing blocks were then processed, and paraffin sections (8–10 μm) were prepared for staining for iPLA$_2\beta$ and SREBP-1. The sections were incubated overnight with primary antibodies (1:25), washed with PBS (4 × 30 min), incubated for 2–3 h with secondary antibodies (1:100 of Cy3 for iPLA$_2\beta$ and Alexa Fluor 594 for SREBP-1), and washed with PBS (three times for 10 min each). DAPI stain (20–30 μl) was then added, and the sections were sealed with a coverslip using nail polish.

Statistical Analyses—Data were converted to mean ± S.E. values, and Student's *t* test was applied to determine significant differences between two samples ($p < 0.05$). The *n* value for each analysis is indicted in the figure legends.

RESULTS

Expression of ER Stress Factors in Akita β-Cells—As part of the unfolded protein response, various ER factors are induced to alleviate ER stress. One such marker of unfolded protein response activation is pPERK (51). Because the Akita β-cells are reported to be a spontaneous model of ER stress, we compared pPERK levels in these cells with those in WT β-cells. As shown in Fig. 1, basal pPERK is greater in the Akita relative to wild type cells. Although exposure to thapsigargin induced pPERK expression in both the WT and Akita cells, they peaked earlier and remained higher in the Akita cells (Fig. 1*B*). These observations are consistent with the original findings of increased ER molecular chaperones and ER stress response element-binding transcription factors in the Akita cells (43) and confirm that the Akita cells are predisposed to developing ER stress and that they are a good model for the study of underlying mechanisms that contribute to β-cell apoptosis due to ER stress.

Reduced Sphingomyelins in Akita β-Cells—We reported that ER stress-induced ceramide generation via NSMase-catalyzed sphingomyelin hydrolysis was a critical contributor to INS-1 cell apoptosis (41, 42). If this pathway is activated by ER stress, this should be reflected by reduced abundances of sphingomyelin molecular species in the Akita cells. To examine this possibility, WT and Akita cells were harvested under basal conditions and analyzed by ESI/MS/MS. The spectra in Fig. 2 display tracings of Li^+ adducts of sphingomyelin species in cell lysates after the addition of the 14:0/14:0-GPC internal standard, which is represented in the spectrum by its $(M + Li^+)^+$ ion (*m/z* 684). Similar to the INS-1 cells, the major sphingomyelin species endogenous to WT and Akita β-cells are 16:0 (*m/z* 709), 18:0 (*m/z* 737), 22:0 (*m/z* 693), 24:1 (*m/z* 819), and 24:0 (*m/z* 821). The spectra were acquired by monitoring constant neutral loss of 59, as described (52), in WT (Fig. 2*A*) and Akita (Fig. 2*B*) cells. As reflected by the decreases in the intensity of ions representing them, the relative abundances of the sphingomyelin molecular species are decreased in the Akita cells in comparison with WT cells. Normalization of individual sphingomyelin molecular species to lipid phosphorus revealed the 16:0, 18:0, 22:0, 24:0, and 24:1 species in the Akita cells to be 47 ± 9, 22 ± 2, 75 ± 4, 95 ± 4, and 78 ± 10% of WT cells, respectively. The total pool of sphingomyelins (pmol/μmol of PO_4) revealed a 48% decrease in sphingomyelin abundance in the Akita cells, relative to the WT cells (Fig. 2*C*). These findings indicate that hydrolysis of sphingomyelins is ramped up in the Akita cells and suggest the possibility of consequential triggering of mitochondrial abnormalities.

Compromised ΔΨ in Akita β-Cells—Loss of ΔΨ is an important step in the induction of cellular apoptosis (47). Because thapsigargin-induced ER stress caused a loss in INS-1 cell ΔΨ

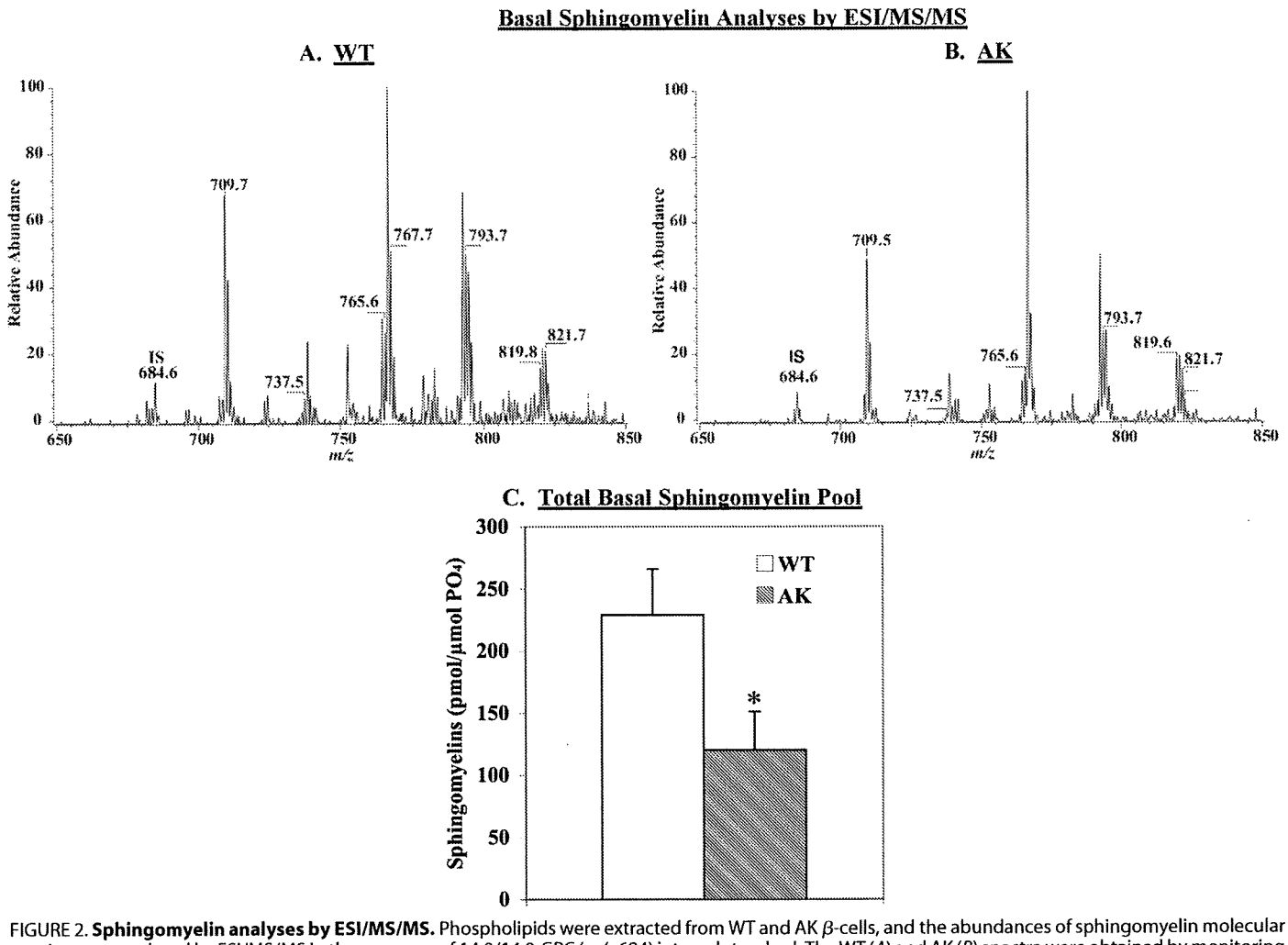

FIGURE 2. **Sphingomyelin analyses by ESI/MS/MS.** Phospholipids were extracted from WT and AK β-cells, and the abundances of sphingomyelin molecular species were analyzed by ESI/MS/MS in the presence of 14:0/14:0-GPC (*m/z* 684) internal standard. The WT (*A*) and AK (*B*) spectra were obtained by monitoring constant neutral loss of 59. *C*, total sphingomyelin pool. Content of each sphingomyelin molecular species (pmol) was determined in each group and normalized to total phosphate (μmol of PO_4). The means ± S.E. (n = 3) of the total (pmol/μmol of PO_4) sphingomyelin pools are presented. *, AK group significantly different from WT, $p < 0.05$.

(42) in an NSMase-dependent manner, we examined whether there was a similar compromising of ΔΨ in the Akita cells. As in the earlier study, we used a flow cytometry protocol to monitor ΔΨ in a suspension of cells to which a fluorescent Mito Flow reagent was added. This reagent concentrates in the mitochondria of healthy cells, but the mitochondria of cells undergoing apoptosis become compromised and accumulate less of the reagent, and this is reflected by a decrease in the fluorescence signal and the appearance of a second peak that is left of the original. The spectra presented in Fig. 3*A* reflect fluorescence measurement in 10,000 cells, and the percentage of cells (mean of four separate experiments) losing ΔΨ was analyzed by the application software and is indicated as *M1*. These analyses revealed that a higher percentage of Akita cells have compromised ΔΨ than WT cells under basal conditions. However, unlike the INS-1 cells, the Akita and corresponding WT cells were found to be prone to clumping. This resulted in broader peaks in the spectra and an unexpectedly higher *M1* value, even in the WT cells. We therefore established a second protocol in which mitochondria-associated $DiOC_6(3)$ staining (*green*) was monitored in live cells by confocal microscopy. As seen in Fig. 3*B*, $DiOC_6(3)$ under basal conditions is more significantly retained in the mitochondria of WT than in Akita cells, confirming compromised mitochondrial integrity in the Akita cells. Further, Hoechst staining (*blue*) reveals that the nuclei in Akita cells are irregular in shape and size, as compared with the nuclei in WT cells, suggesting that the cell death process is under way in the Akita cells. These findings suggest that the spontaneous development of ER stress in β-cells also triggers the mitochondrial apoptotic pathway.

Basal and ER Stress-induced Apoptosis Are Amplified in Akita β-Cells—In view of the above findings, we next examined if the Akita cells are more susceptible to apoptosis. TUNEL analyses (Fig. 4*A*) revealed a higher incidence of basal apoptosis that was coincident with higher levels of activated caspase-3 (Fig. 4, *B* and *C*). Exposure to thapsigargin induced activation of caspase-3 in both wild type and Akita with peak activation achieved earlier in the Akita cells than in the wild type cells. This is reflected by a greater -fold increase, relative to basal, in Akita cell apoptosis at 8 h (WT, 1.59 ± 0.09 *versus* Akita (AK), 2.26 ± 0.16, $p = 0.0175$).

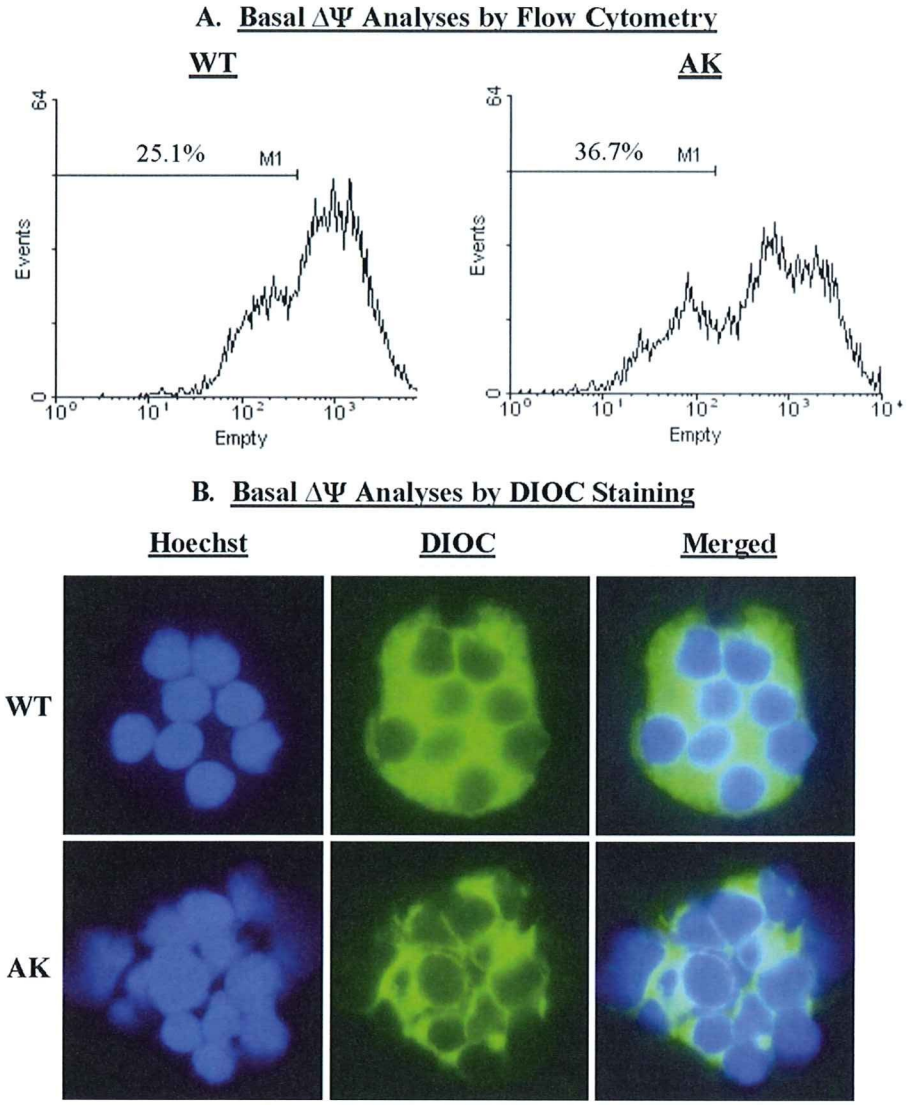

FIGURE 3. **Basal mitochondrial membrane potential (ΔΨ) monitoring.** ΔΨ was monitored in WT and AK β-cells by flow cytometry and DiOC$_6$(3) staining. *A*, flow cytometry. The spectra reflect fluorescence measurement in 10,000 cells, and the percentage of cells losing ΔΨ is indicated as *M1*. These analyses were done four separate times. *B*, DiOC$_6$(3) staining. Cells were loaded with the *blue* nuclear (Hoechst; *left panels*) and *green* mitochondrial (DiOC$_6$(3) (*DIOC*); *middle panels*) stain and examined by confocal microscopy. The *merged images* are shown in the *right panels*.

ER Stress Amplifies ΔΨ Loss in Akita β-Cells—Because induction of ER stress led to mitochondrial abnormalities in the INS-1 cells, we examined whether a similar affect was evident in the Akita cells. Compared with basal conditions (Fig. 2*B*), exposure to thapsigargin for 8 h resulted in dispersion of DiOC$_6$(3) staining and loss in nuclear uniformity in the WT cells (Fig. 4*D*). These outcomes were accelerated in the Akita cells and suggest that activation of the mitochondrial apoptotic pathway contributes to ER stress-induced apoptosis of these cells also.

Expression and ER Stress-induced Activation of iPLA$_2$β and NSMase—Our collective observations (40–42) indicate that ER stress-induced apoptosis occurs by an iPLA$_2$β-dependent mechanism involving induction of NSMase and activation of the mitochondrial apoptotic pathway. The above findings suggest participation of both NSMase and the mitochondria in Akita β-cell death. We therefore examined the extent of the iPLA$_2$β role in this process. Surprisingly, basal expression of iPLA$_2$β protein was found to be greater in the Akita than in the WT cells (Fig. 5*A*), and this was reflected by a 3-fold higher activity (16 ± 1 pmol/mg of protein/min for WT *versus* 54 ± 3 pmol/mg of protein/min for Akita). Also, as shown in Fig. 5*B*, exposure to thapsigargin promoted iPLA$_2$β activity in both WT and AK β-cells. Consistent with manifestation of an iPLA$_2$β activity, basal and thapsigargin-treated activities were suppressed by BEL and stimulated by ATP (~3-fold) in WT and AK β-cells.

Because we previously reported iPLA$_2$β-mediated induction of NSMase during ER stress, we compared its message levels in the WT and Akita cells. As shown in Fig. 5*C*, basal NSMase was higher in the Akita than in the WT cells, and exposure to thapsigargin induced NSMase. The increase in NSMase message occurred earlier and reached a higher -fold increase in the Akita cells, relative to WT cells. Consistent with an iPLA$_2$β-mediated effect, NSMase induction in both groups was inhibited by inactivation of iPLA$_2$β with BEL.

In contrast with the earlier observations in INS-1 cells, in which iPLA$_2$β was overexpressed (41, 42) and the cells were treated with thapsigargin, the responses described here in the Akita β-cells occurred in a spontaneous ER stress model. The present findings therefore strengthen the likelihood that iPLA$_2$β plays a critical role in ER stress-induced β-cell apoptosis.

Evidence for Induction of iPLA$_2$β by SREBP-1 during ER Stress—The finding of increased iPLA$_2$β expression in the Akita cells suggests that the β-cell iPLA$_2$β may be subject to regulation, but the mechanism for its induction remains to be elucidated. One potential possibility is suggested by the recent report identifying a sterol-regulatory element (SRE) in the iPLA$_2$β gene (53). That study performed in Chinese hamster ovary cells revealed that binding of SREBPs to SRE leads to iPLA$_2$β transcription. Of relevance to our interests is that SREBPs are known to be induced under stressful conditions and processed to the mature form of SREBPs (mSREBP) in β-cells experiencing ER stress due to glucolipotoxicity and thapsigargin (54). Consistent with these observations, we find that basal expression of mSREBP-1 protein is greater in Akita than in WT cells (Fig. 6*A*). Further, Akt phosphorylation, which promotes SREBP-1 processing

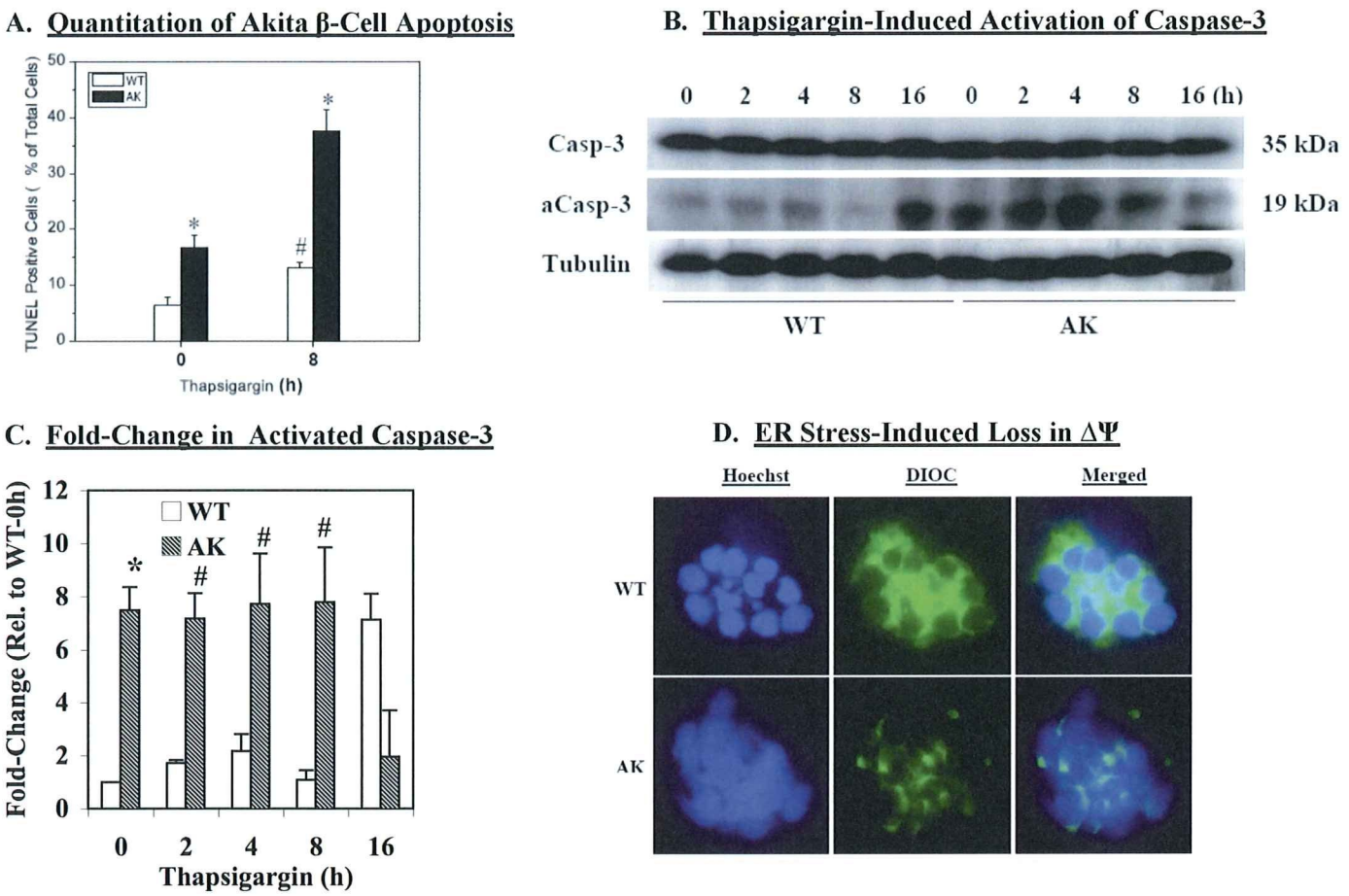

FIGURE 4. **Assessment of apoptosis and mitochondrial membrane potential (ΔΨ) in Akita β-cells.** WT and AK β-cells were exposed to DMSO (control) or thapsigargin (*T*) (0.50 μM) and harvested at various times for analyses. *A*, apoptosis quantitation. Total cell number was determined using DAPI nuclear stain, and the mean ± S.E. ($n = 3$) percentages of TUNEL-positive apoptotic cells are presented. *, AK group significantly different from WT, $p < 0.05$. #, WT treated group significantly different from WT control group, $p < 0.05$. *B*, caspase-3 activation. Cell lysates were prepared and processed for full-length and activated caspase-3 (*Casp-3* and *aCasp-3*, respectively) immunoblotting analyses. Tubulin was used as a loading control. These analyses were done three separate times. *C*, activated caspase-3 densitometry. The ratio of the activated caspase-3-immunoreactive band to the corresponding tubulin band was determined, and means ± S.E. of -fold change relative to WT at 0 h are presented. * and #, significantly different from corresponding WT; $p < 0.01$ and $p < 0.05$, respectively. *D*, ΔΨ analyses. Following exposure to DMSO or thapsigargin for 8 h, the WT and AK β-cells were loaded with the blue nuclear (Hoechst) (*left panels*) and green mitochondrial ($DiOC_6(3)$) (*DIOC*) (*middle panels*) stains and examined by confocal microscopy. The *merged images* are shown in the *right panels*.

and nuclear accumulation of the mSREBP-1 (55–57), is also increased.

To determine if there is a link between SREBP-1 and iPLA$_2$β expression, cells were treated with thapsigargin and harvested at various times for immunoblotting analyses. Exposure to thapsigargin promoted a temporal increase in iPLA$_2$β expression in both WT and Akita cells (Fig. 6*B*), with a more pronounced and earlier increase apparent in the Akita cells. Also, as seen in Fig. 6*C*, corresponding increases in mSREBP-1 and pAkt are also evident. These findings reveal a correlation between iPLA$_2$β and generation of SREBP-1; however, they do not indicate whether the increase in iPLA$_2$β expression is due to SREBP-1 processing.

To address a direct role of SREBP-1 on iPLA$_2$β induction, we expressed a DN form of SREBP-1 in the WT and Akita cells. It has been reported that although the DN form itself is unable to activate transcription, it interferes with the processing of endogenous SREBP-1 and its binding to the SRE element (49). As seen in Fig. 6*D*, expression of the DN SREBP-1 reduced basal levels of the mSREBP-1 form and its increase following exposure to thapsigargin. In association with the reduction in mSREBP-1, both basal and thapsigargin-induced increases in iPLA$_2$β were suppressed in cells expressing the DN SREBP-1 (Fig. 6*E*). As expected by the upstream role of pAkt in SREBP-1 activation, phosphorylation of Akt was unaffected by DN SREBP-1 (data not shown). These findings are taken to indicate that SREBP-1 activation can promote iPLA$_2$β expression.

Effects of iPLA$_2$β Knockdown in the Akita Cells—Because basal iPLA$_2$β is increased in the Akita cells that are predisposed to developing ER stress and is induced in both WT and Akita cells following exposure to thapsigargin, we next examined whether suppression of iPLA$_2$β expression prevents the observed outcomes. To address this issue, we used siRNA protocols to knockdown iPLA$_2$β in the WT and Akita cells. The cells were harvested under basal conditions or following an 8-h exposure to thapsigargin. As illustrated in Fig. 7*A*, both basal and thapsigargin-induced iPLA$_2$β protein expression are reduced in the WT and Akita cells transfected with the iPLA$_2$β siRNA (*si*), relative to cells transfected with the control siRNA (*si**). Comparison of iPLA$_2$β message in the control siRNA-transfected WT and Akita cells revealed nearly 2.5-fold higher basal iPLA$_2$β message in the Akita cells (Fig. 7*B*). Transfection

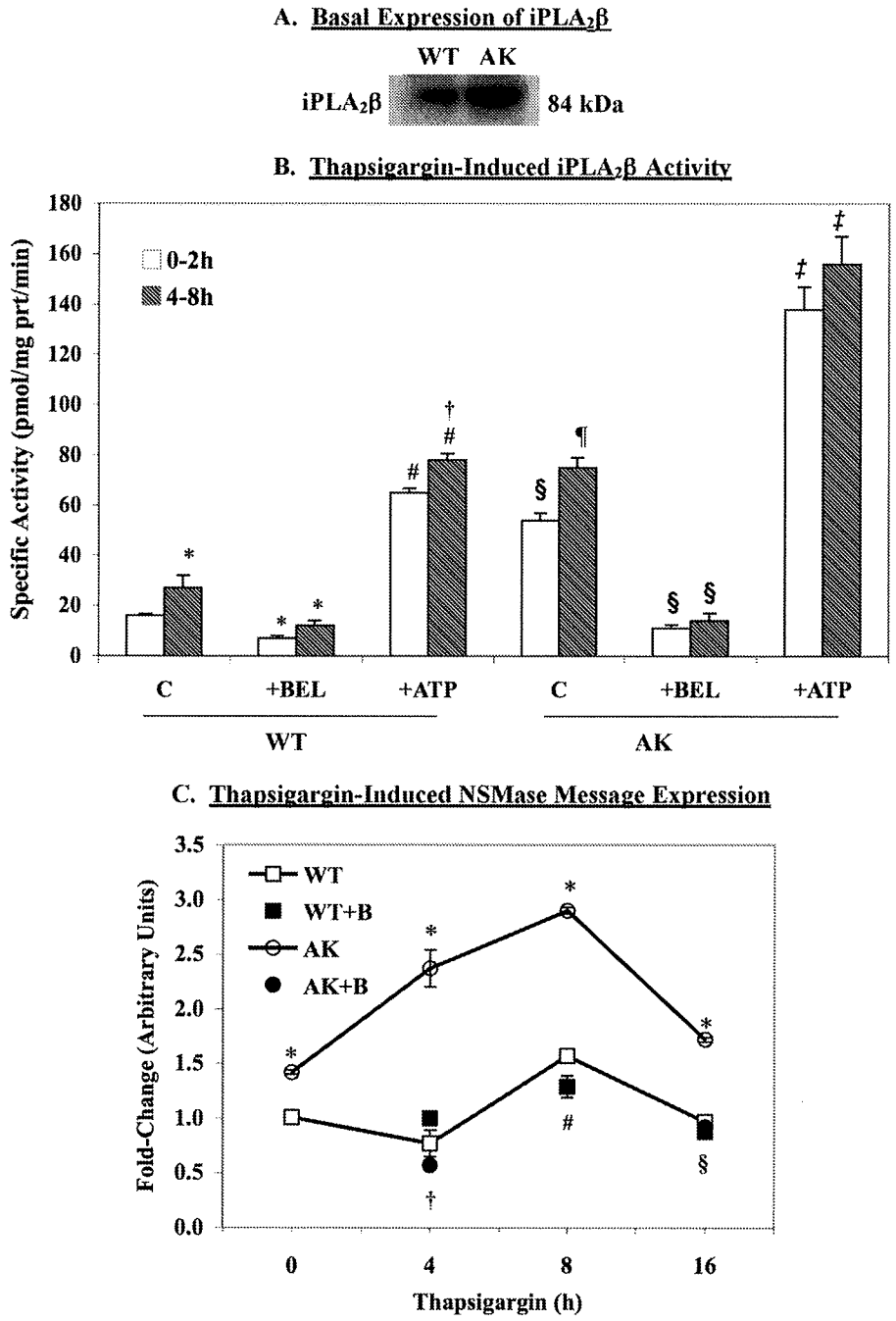

FIGURE 5. **Basal and ER stress-induced expression of iPLA$_2$β and NSMase.** *A*, iPLA$_2$β protein. Cell lysates were prepared from WT and AK β-cells, and 30-μg protein aliquots were processed for immunoblotting analyses. *B*, iPLA$_2$β activity. Cytosol was prepared from control or thapsigargin-treated (0.50 μM) AK cells, and iPLA$_2$β catalytic activity was assayed in 25 μg of cytosolic protein in the absence and presence of ATP (10 mM) or BEL (1 μM). Means ± S.E. (n = 6–8) of specific activity (pmol/mg protein/min) are presented. *, WT 4–8 h significantly different from WT 0–2 h and WT with BEL significantly different from corresponding WT without BEL, $p < 0.05$. #, WT with ATP significantly different from corresponding WT without ATP, $p < 0.0001$. †, WT with ATP 4–8 h significantly different from WT 0–2 h, $p < 0.005$. §, AK 0–2 h significantly different from WT 0–2 h and AK with BEL significantly different from corresponding AK without BEL, $p < 0.0001$. ¶, AK 4–8 h significantly different from AK 0–2 h, $p < 0.001$. ‡, AK with ATP significantly different from AK without ATP, $p < 0.00001$. *C*, NSMase message. Total RNA was isolated from DMSO- or thapsigargin-treated (0–16 h) WT and AK β-cells, and qRT-PCR analyses were performed for NSMase. In some experiments, the cells were treated with BEL (+*B*) (1 μM) for 30 min, washed, and then exposed to thapsigargin. Means ± S.E. (n = 5–6) of the -fold increase in message are presented. 18 S was used as a housekeeping control. *, AK significantly different from corresponding WT, $p < 0.0005$. †, AK with BEL significantly different from AK, $p < 0.001$. #, WT with BEL significantly different from WT, $p < 0.05$. §, AK with BEL significantly different from AK, $p < 0.05$.

of the Akita cells with the iPLA$_2$β siRNA reduced basal iPLA$_2$β message levels and prevented iPLA$_2$β induction due to thapsigargin.

Basal NSMase message levels that were higher in non-transfected Akita cells (Fig. 5*C*) remained greater in the Akita, relative to wild type, cells transfected with the control siRNA (arbitrary units 1.01 ± 0.06 for WT *versus* 2.09 ± 0.40 for AK, $p = 0.0171$). Although transfection with the iPLA$_2$β siRNA did not alter basal NSMase message levels, it significantly suppressed thapsigargin-induced increase in NSMase message (Fig. 7*C*).

To obtain a measure of a role for iPLA$_2$β in promoting loss in mitochondrial ΔΨ, the cells were processed by flow cytometry. This allowed quantitative assessment of the number of cells with compromised ΔΨ. The incidence of loss in ΔΨ under untransfected basal conditions was greater in the Akita, relative to wild type, cells (22 ± 2% for WT *versus* 33 ± 2% for AK, $p = 0.0185$). As shown in Fig. 7*D*, transfection with control or iPLA$_2$β siRNAs did not significantly affect the basal incidence of cells with ΔΨ loss, but iPLA$_2$β siRNA prevented thapsigargin-induced increase in the percentage of Akita cells that lose ΔΨ.

The effect of suppressing iPLA$_2$β expression on the final outcome of apoptosis was tested next using TUNEL analyses. As shown in Fig. 7*E*, transfection with control siRNA did not suppress the higher incidence of apoptosis in Akita cells, relative to WT cells (see Fig. 4*A*). However, transfection with iPLA$_2$β siRNA suppressed basal apoptosis and also prevented thapsigargin-induced apoptosis in the Akita cells. These findings are taken as direct evidence of an important role for iPLA$_2$β in the apoptosis process induced by ER stress in β-cells.

iPLA$_2$β, SREBP-1, and NSMase Messages and iPLA$_2$β and SRE-binding Protein in Islets from Akita Mice—In light of the observations in the Akita β-cells, we considered whether iPLA$_2$β and SREBP-1

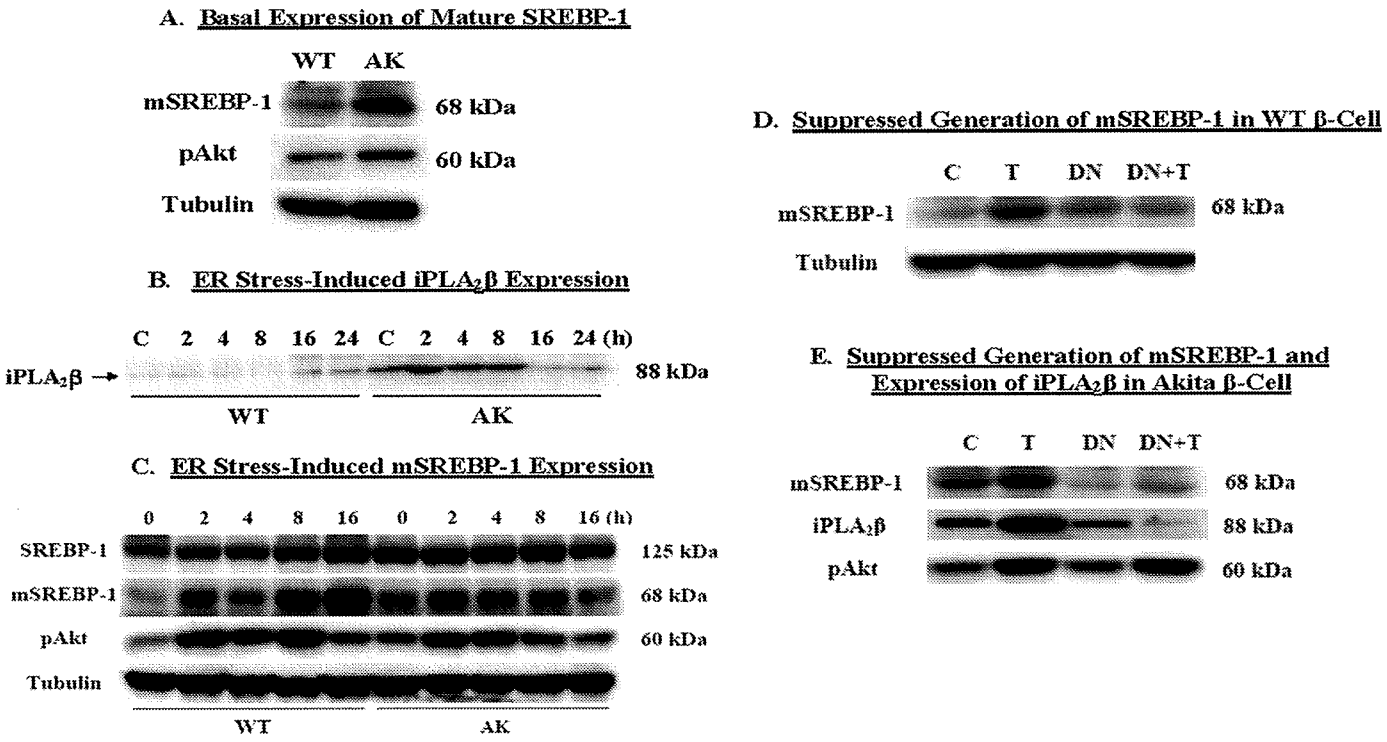

FIGURE 6. **SREBP-1 expression and SREBP-1-induced activation of iPLA$_2$β.** WT and AK β-cells were exposed to DMSO (*Control*) or thapsigargin (*T*) (0.50 μM) and harvested at various times, and 30-μg protein aliquots were processed for immunoblotting analyses. *A*, basal mSREBP-1 expression. *B*, thapsigargin-induced iPLA$_2$β expression. *C*, thapsigargin-induced mSREBP-1 expression. DN SREBP-1 was expressed in WT and AK β-cells and treated with DMSO or thapsigargin (0.50 μM) for 8 h. Cell lysates were then prepared, and 30-μg protein aliquots were processed for immunoblotting analyses for mSREBP-1 and iPLA$_2$β. *D*, mSREBP-1 in WT β-cells. *E*, mSREBP-1 and iPLA$_2$β in Akita β-cells. Tubulin was used as a loading control. These analyses were done 3–5 separate times.

expression is altered under *in vivo* conditions in the Akita mouse model. We therefore isolated islets from Akita and WT littermates and prepared cDNA for qRT-PCR analyses. The mice were sacrificed within a week of weaning (4–5 weeks of age). Even at this early age, the Akita mice exhibited hyperglycemia (~450 mg/dl), whereas the WT mice were euglycemic. Consistent with the findings in the Akita cells, mRNAs for iPLA$_2$β, SREBP-1, and NSMase were significantly elevated in the Akita islets, relative to WT islets (Fig. 8*A*).

To substantiate the findings of higher message in the Akita islets, we performed immnocytofluorescence analyses for iPLA$_2$β and SREBP-1. Paraffin sections (10 μm) of islets were prepared and stained for nucleus-associating DAPI (*blue*) and iPLA$_2$β or SREBP-1 (*red*). The exposure times for each were the same in WT and AK sections. Whereas diffuse background fluorescence was evident in the WT islets, intense and punctate staining of SREBP-1 (Fig. 8*B*) and iPLA$_2$β (Fig. 8*C*) are seen in the Akita islets. These findings are taken as evidence for increased expression of both SREBP-1 and iPLA$_2$β in islets from diabetic Akita mice, relative to islets from age-matched normoglycemic WT mice. Similar to the observations in the Akita β-cells above, the Akita islet cell nuclei were also irregular in shape with some evidence of fragmentation in comparison with the rounded and uniform structure of the nuclei in WT islets (*insets* in the *left panels* of Fig. 8*B*). Our findings in Akita islets thus reveal the potential activation of a pathway linking SREBP-1, iPLA$_2$β, and NSMase in an animal model that develops diabetes as a consequence of β-cell apoptosis resulting from spontaneous development of ER stress in islet β-cells.

DISCUSSION

Both T1DM and T2DM are associated with losses in β-cells due to apoptosis. It is therefore important to determine the underlying mechanisms that contribute to this process. Recent reports in experimental models and in clinical settings suggest that ER stress is a potential cause of β-cell apoptosis during the development of diabetes mellitus (6, 15–22, 24–26). Because β-cells serve a secretory function, they are endowed with a highly developed ER that renders them particularly susceptible to developing ER stress.

We found that ER stress causes INS-1 cell apoptosis, in part, by an iPLA$_2$β-dependent mechanism (40). Subsequent studies revealed a previously unrecognized pathway (41, 42) involving accumulation of ceramides via an iPLA$_2$β-mediated induction of NSMase. The ceramides, generated from NSMase-catalyzed hydrolysis of sphingomyelins, promote mitochondrial abnormalities and amplify the apoptosis outcome. The roles for iPLA$_2$β and NSMase in this process are supported by the findings of suppression of sphingomyelin hydrolysis, ceramide generation, mitochondrial activation, and apoptosis following inactivation of iPLA$_2$β or NSMase (41, 42).

The above proposed schema of iPLA$_2$β involvement in β-cell apoptosis was derived from studies in INS-1 cells in which ER stress was induced with thapsigargin. The plausibility of the pathway is strengthened by the finding that it is amplified by overexpression of iPLA$_2$β and suppressed by inactivation of iPLA$_2$β. However, identification of a similar role for iPLA$_2$β in a spontaneous ER stress model would significantly strengthen

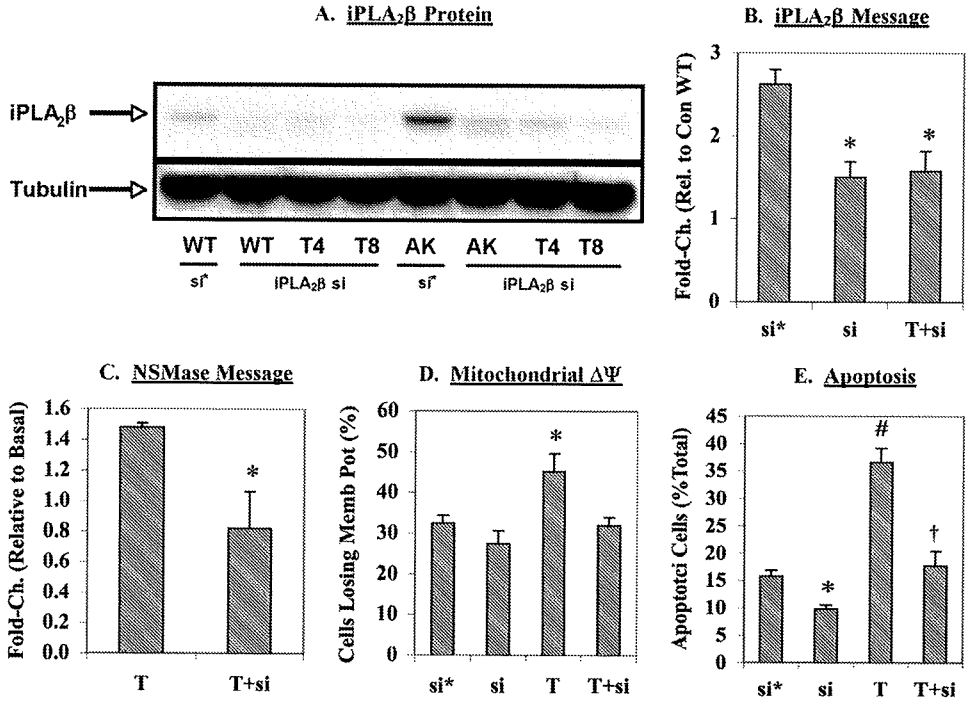

FIGURE 7. **Effects of iPLA$_2$β knockdown on NSMase induction, mitochondrial membrane potential loss, and apoptosis in Akita cells.** Wild type and Akita cells were transfected with either control siRNA (*si**) or iPLA$_2$β siRNA (*si*) and subsequently treated with DMSO vehicle or thapsigargin (*T*) (1 μM). The cells were harvested at 8 h for various experimental protocols, each done 3–5 times. *A*, iPLA$_2$β protein. Cell lysates were prepared, and 30-μg protein aliquots were processed for immunoblotting. *B*, iPLA$_2$β message. Total RNA was prepared, and cDNA was generated for qRT-PCR of iPLA$_2$β message. *, significantly different from the control siRNA group, $p < 0.01$. *C*, NSMase message. Total RNA was prepared, and cDNA was generated for qRT-PCR of NSMase message. *, significantly different from the thapsigargin group, $p < 0.05$. *D*, mitochondrial membrane potential. The percentage of cells losing ΔΨ was determined using the flow cytometry protocol as described for Fig. 3. *, significantly different from all other groups, $p < 0.05$. *E*, apoptosis. The incidence of cell death was assessed using the TUNEL assay. *, iPLA$_2$β siRNA group significantly different from the control siRNA group, $p < 0.001$. #, thapsigargin group significantly different from the control siRNA group, $p < 0.0001$. †, thapsigargin plus iPLA$_2$β siRNA group significantly different from the thapsigargin group, $p < 0.005$. The means ± S.E. for each measurement are presented in *B–E*.

the assertion that iPLA$_2$β participates in ER stress-induced β-cell apoptosis. We therefore chose to address this issue in the Akita mouse model. However, because the islet yield from these mice is limiting, we pursued studies in a β-cell line established from the Akita mice (43). The findings in these cells were compared with a β-cell line derived from isogenic WT littermates.

Herein, we find that even under basal conditions, the Akita β-cells are predisposed to developing ER stress, as reflected by the greater induction of pPERK, and to be more prone to undergo apoptosis, as revealed by the greater abundance of TUNEL-positive cells and activated caspase-3, relative to WT β-cells. The greater propensity of the Akita cells to develop ER stress under basal conditions is also revealed by the nearly 2-fold higher basal splicing of XBP1 mRNA in the Akita cells, relative to isogenic WT counterparts (58).

The Akita cells also expressed higher message for NSMase, contained lower abundances of sphingomyelins, and exhibited a higher incidence of loss in mitochondrial membrane potential (ΔΨ). Permeabilization of the outer mitochondrial membrane is considered to be a "point of no return" during apoptosis (59), and PTP opening alters outer mitochondrial membrane permeability. Prolonged activation of PTP leads to loss in ΔΨ and release of cytochrome *c*, a necessary event in the mitochondrial cell death pathway (60, 61), from the mitochondrial intermembrane space into the cytosol. Following its release into the cytosol, the proapoptotic cytochrome *c* forms the apoptosome complex with apoptosis protease-activating factor-1 to induce caspases and subsequent apoptosis (62). The present findings therefore are consistent with the triggering of mitochondrial abnormalities as a consequence of increased sphingomyelin hydrolysis in Akita β-cells (41, 42).

Most intriguingly, the Akita cells expressed higher iPLA$_2$β protein than the WT cells. This was reflected by a nearly 3-fold higher basal cytosolic iPLA$_2$β specific activity. These findings strengthen the likelihood that iPLA$_2$β-mediated NSMase activation is a critical factor in ER stress-induced β-cell apoptosis. To further establish this possibility, the effects of accelerating ER stress in the Akita cells were assessed. Exposure to thapsigargin caused elevations in caspase-3 activation and abundance of TUNEL-positive cells that were accompanied by temporal increases in iPLA$_2$β protein and specific activity in both WT and Akita β-cells. However, these outcomes were accelerated in the Akita cells. Thapsigargin also induced NSMase in both WT and Akita cells, and this occurred earlier and the -fold increases in message were greater in the Akita cells. That this was an iPLA$_2$β-dependent effect was evidenced by the suppression in NSMase induction following inactivation of iPLA$_2$β in both WT and Akita cells.

To establish that the outcomes measured in the Akita β-cells require iPLA$_2$β, the Akita cells were transfected with iPLA$_2$β siRNA to knock down iPLA$_2$β message and protein levels. The siRNA protocol resulted in dramatic suppression of not only basal but also thapsigargin-induced increases in iPLA$_2$β message and protein. Further, whereas thapsigargin-induced NSMase induction, mitochondrial membrane potential loss, and apoptosis were unaffected by transfection with control siRNA, they were significantly suppressed in Akita cells transfected with the iPLA$_2$β siRNA. In fact, the higher basal apoptosis was also significantly decreased in these cells. These findings indicate that iPLA$_2$β is a critical factor during the development and progression of ER stress-induced abnormalities in the β-cell.

Our recent finding of higher iPLA$_2$β protein and activity in the ER and mitochondria of INS-1 cells exposed to thapsigargin was suggestive of increased mobilization of iPLA$_2$β by these organelles with the onset and development of ER stress (41, 42). However, the surprising finding of higher basal iPLA$_2$β protein

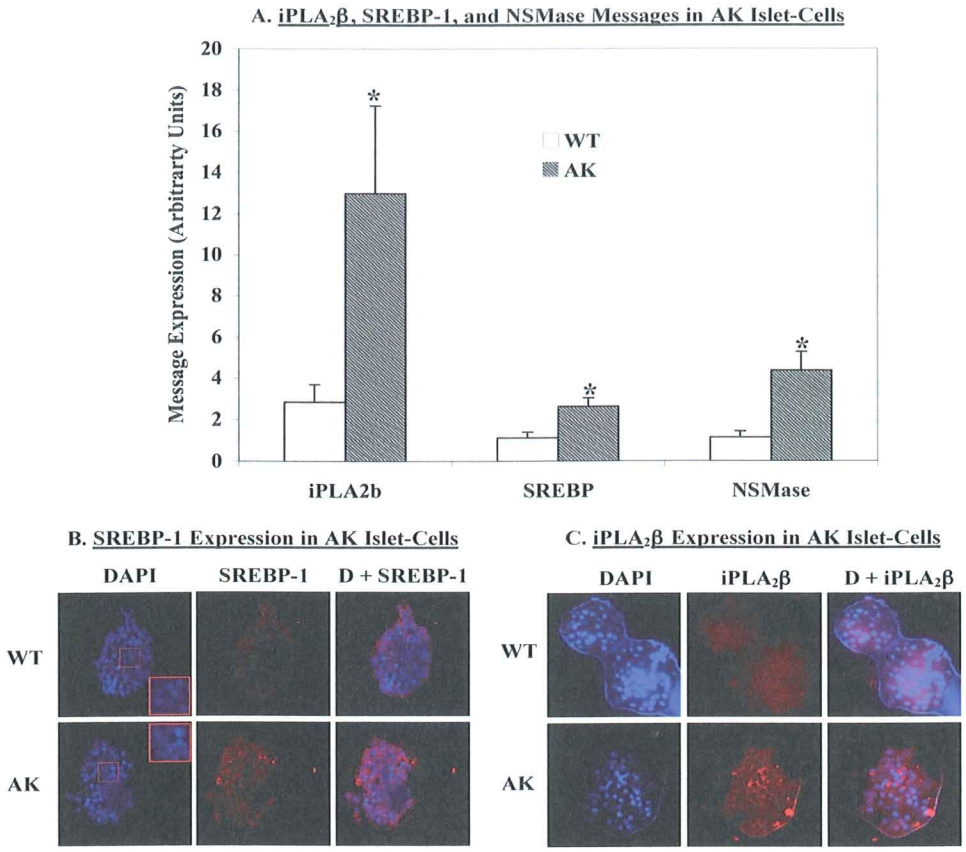

FIGURE 8. **iPLA$_2$β, SREBP-1, and NSMase message and iPLA$_2$β and SREBP-1 protein expression in Akita mouse islets.** Islets were isolated from WT and Akita mice at 4 weeks of age. Total RNA was prepared, and qRT-PCR analyses for iPLA$_2$β, SREBP-1, and NSMase were performed. Means ± S.E. (n = 3–5) of the -fold increase in each message are presented (*A*). 18 S was used as a control. *, AK group significantly different from corresponding WT group, $p < 0.05$. *B* and *C*, paraffin sections (10 μm) of islets isolated from WT and AK mice at ~4 weeks of age were prepared and stained for cell nuclei (DAPI) (*blue*) and SREBP-1 (*red* in *B*) or iPLA$_2$β (*red* in *C*), and fluorescence was recorded using a Nikon Eclipse TE300 microscope. The *insets* in *B* are magnifications of islet cell nuclei.

expression in Akita cells in the present study raises the possibility that it may in fact be subject to pre- and post-transcriptional regulation under stressful conditions.

Other than ATP, only two potential candidates have been identified as regulating iPLA$_2$β: CaMKIIβ and SREBP-1. Whereas CaMKIIβ is reported to activate iPLA$_2$β (63), SREBP-1 has been shown to promote transcription of the iPLA$_2$β gene (53). The transcription factor ATF6 plays a key role in the unfolded protein response, and ER stress leads to its cleavage by site 1 and site 2 proteases that are also activated by ER stress (64). These proteases process SREBPs (65) into active mature forms that enter the nucleus and transactivate target genes (66). SREBPs are known to be induced under stressful conditions and are activated in β-cells experiencing ER stress due to glucolipotoxicity or thapsigargin (54). A fascinating extension to these observations is the recent identification of an SRE in the iPLA$_2$β gene (53). That study, performed in Chinese hamster ovary cells that were mutated to constitutively generate mSREBPs, revealed that binding of mSREBPs to SRE leads to iPLA$_2$β transcription. We therefore considered the possibility that SREBP-1 may modulate iPLA$_2$β levels in β-cells that are predisposed to developing ER stress.

We find that processing of SREBP-1 to the mSREBP-1 form under basal conditions is higher in the Akita β-cells than in the WT β-cells. This coincided with higher pAkt levels, which is consistent with previous reports that phosphorylation of Akt stimulates the synthesis and nuclear localization of mSREBP-1 (55–57). Further, exposure to thapsigargin led to temporal increases in mSREBP-1 (and pAkt) in parallel with elevations in iPLA$_2$β protein. These findings provide the first evidence of a correlation between mSREBP-1 and iPLA$_2$β expression with the onset and progression of diminished cellular integrity.

To determine if there is a causal relationship between SREBP-1 activation and iPLA$_2$β expression, a DN SREBP-1 was expressed in WT and Akita β-cells. The DN form itself is unable to activate transcription, but it interferes with the processing of endogenous SREBP-1 and its binding to the SRE element (49). As expected, both basal and thapsigargin-induced increase in mSREBP-1 were suppressed in WT and Akita cells by DN-SREBP-1, whereas phosphorylation of Akt, an event upstream of SREBP-1, remained unaffected. Also, consistent with mSREBP-1-mediated regulation of iPLA$_2$β expression, both basal and induced iPLA$_2$β expression were suppressed by the DN protein.

These observations therefore identify a novel mechanism by which a biological process (stress) can regulate iPLA$_2$β expression in β-cells. Because of accumulating evidence supporting a causative role for ER stress-induced β-cell apoptosis in the development of diabetes, we sought to substantiate our findings in the Akita (*Ins2Akita*) mouse. These mice develop mild hyperglycemia rapidly after birth, although they continue to live for over 8 months. These mice contain a spontaneous dominant mutation in the insulin 2 gene on a C57BL6 mouse background that results in the replacement of cysteine with tyrosine at position 96, causing disruption of a disulfide bridge required for proper insulin folding. This causes proinsulin to accumulate in the ER and leads to the initiation of the unfolded protein response. The unresolved ER stress subsequently leads to pancreatic islet β-cell apoptosis in the absence of obesity, insulitis, or insulin resistance (45, 67–70). Heterozygous Akita mice become hyperglycemic at 3–4 weeks of age but remain fertile and viable in the absence of exogenous insulin treatment. The diabetic phenotype is more severe and progressive in the Akita male than in the female. We therefore examined islets from male Akita and WT littermates of ~4 weeks of age.

Consistent with the findings in the Akita β-cells, iPLA$_2$β, SREBP-1, and NSmase messages were significantly increased in

the Akita islets, as compared with WT islets. This was supported by the more prominent staining for iPLA$_2\beta$ and SREBP-1 in Akita, relative to the WT, islet sections. It may be argued that the SREBP-1 detected does not appear to be nucleus-associated. However, typically, only a fraction of the total SREBP-1 pool is processed to the mature form that translocates to the nucleus. Although others have demonstrated nuclear translocation by immunocytochemistry (48, 49), these studies were performed with overexpressed truncated SREBP1. As such, it is likely that the immunocytochemistry assay is not sufficiently sensitive to detect translocation of endogenous SREBP1. Nevertheless, collectively, these findings strongly support a link between and a role for SREBP-1, iPLA$_2\beta$, and NSMase during the development of diabetes mellitus due to ER stress-induced in β-cell apoptosis.

Multiple lines of evidence indicate that the loss of β-cells due to apoptosis contributes to the onset and progression of T1DM and T2DM. It is now recognized that prolonged ER stress can cause β-cell apoptosis and lead to the development of diabetes mellitus, and we recently identified a role for iPLA$_2\beta$ in ER stress-induced β-cell apoptosis. Here, we present evidence for the activation of iPLA$_2\beta$ in a spontaneous ER stress model that leads to the development of diabetes due to β-cell apoptosis. We further identified for the first time that iPLA$_2\beta$ expression is subject to regulation by SREBP-1 during the evolution of a metabolic disorder, the incidence of which continues to rise. As such, our findings contribute to the understanding of iPLA$_2\beta$ biology and may provide insight into developing novel targeted therapeutics to prevent or delay β-cell apoptosis.

Acknowledgments—We acknowledge the advice provided by the Washington University Diabetes Research and Training Center-supported Morphology and β-Cell Morphology cores.

REFERENCES

1. Klöppel, G., Löhr, M., Habich, K., Oberholzer, M., and Heitz, P. U. (1985) *Surv. Synth. Pathol. Res.* **4,** 110–125
2. Stefan, Y., Orci, L., Malaisse-Lagae, F., Perrelet, A., Patel, Y., and Unger, R. H. (1982) *Diabetes* **31,** 694–700
3. Butler, A. E., Janson, J., Bonner-Weir, S., Ritzel, R., Rizza, R. A., and Butler, P. C. (2003) *Diabetes* **52,** 102–110
4. Yoon, K. H., Ko, S. H., Cho, J. H., Lee, J. M., Ahn, Y. B., Song, K. H., Yoo, S. J., Kang, M. I., Cha, B. Y., Lee, K. W., Son, H. Y., Kang, S. K., Kim, H. S., Lee, I. K., and Bonner-Weir, S. (2003) *J. Clin. Endocrinol. Metab.* **88,** 2300–2308
5. Araki, E., Oyadomari, S., and Mori, M. (2003) *Exp. Biol. Med. (Maywood)* **228,** 1213–1217
6. Cardozo, A. K., Ortis, F., Storling, J., Feng, Y. M., Rasschaert, J., Tonnesen, M., Van Eylen, F., Mandrup-Poulsen, T., Herchuelz, A., and Eizirik, D. L. (2005) *Diabetes* **54,** 452–461
7. Mathis, D., Vence, L., and Benoist, C. (2001) *Nature* **414,** 792–798
8. Tisch, R., and McDevitt, H. (1996) *Cell* **85,** 291–297
9. Bernard, C., Berthault, M. F., Saulnier, C., and Ktorza, A. (1999) *FASEB J.* **13,** 1195–1205
10. Pick, A., Clark, J., Kubstrup, C., Levisetti, M., Pugh, W., Bonner-Weir, S., and Polonsky, K. S. (1998) *Diabetes* **47,** 358–364
11. Butler, A. E., Janson, J., Soeller, W. C., and Butler, P. C. (2003) *Diabetes* **52,** 2304–2314
12. Diaz-Horta, O., Kamagate, A., Herchuelz, A., and Van Eylen, F. (2002) *Diabetes* **51,** 1815–1824
13. Rao, R. V., Castro-Obregon, S., Frankowski, H., Schuler, M., Stoka, V., del Rio, G., Bredesen, D. E., and Ellerby, H. M. (2002) *J. Biol. Chem.* **277,** 21836–21842
14. Kaufman, R. J. (1999) *Genes Dev.* **13,** 1211–1233
15. Oyadomari, S., Araki, E., and Mori, M. (2002) *Apoptosis* **7,** 335–345
16. Oyadomari, S., Koizumi, A., Takeda, K., Gotoh, T., Akira, S., Araki, E., and Mori, M. (2002) *J. Clin. Invest.* **109,** 525–532
17. Socha, L., Silva, D., Lesage, S., Goodnow, C., and Petrovsky, N. (2003) *Ann. N.Y. Acad. Sci.* **1005,** 178–183
18. Harding, H. P., Zeng, H., Zhang, Y., Jungries, R., Chung, P., Plesken, H., Sabatini, D. D., and Ron, D. (2001) *Mol. Cell* **7,** 1153–1163
19. Delépine, M., Nicolino, M., Barrett, T., Golamaully, M., Lathrop, G. M., and Julier, C. (2000) *Nat. Genet.* **25,** 406–409
20. Takeda, K., Inoue, H., Tanizawa, Y., Matsuzaki, Y., Oba, J., Watanabe, Y., Shinoda, K., and Oka, Y. (2001) *Hum. Mol. Genet.* **10,** 477–484
21. Fonseca, S. G., Fukuma, M., Lipson, K. L., Nguyen, L. X., Allen, J. R., Oka, Y., and Urano, F. (2005) *J. Biol. Chem.* **280,** 39609–39615
22. Oyadomari, S., Takeda, K., Takiguchi, M., Gotoh, T., Matsumoto, M., Wada, I., Akira, S., Araki, E., and Mori, M. (2001) *Proc. Natl. Acad. Sci. U.S.A.* **98,** 10845–10850
23. Kröncke, K. D., Brenner, H. H., Rodriguez, M. L., Etzkorn, K., Noack, E. A., Kolb, H., and Kolb-Bachofen, V. (1993) *Biochim. Biophys. Acta* **1182,** 221–229
24. Corbett, J. A., and McDaniel, M. L. (1992) *Diabetes* **41,** 897–903
25. Mandrup-Poulsen, T. (1996) *Diabetologia* **39,** 1005–1029
26. Yamada, T., Ishihara, H., Tamura, A., Takahashi, R., Yamaguchi, S., Takei, D., Tokita, A., Satake, C., Tashiro, F., Katagiri, H., Aburatani, H., Miyazaki, J., and Oka, Y. (2006) *Hum. Mol. Genet.* **15,** 1600–1609
27. Schaloske, R. H., and Dennis, E. A. (2006) *Biochim. Biophys. Acta* **1761,** 1246–1259
28. Ma, Z., Ramanadham, S., Wohltmann, M., Bohrer, A., Hsu, F. F., and Turk, J. (2001) *J. Biol. Chem.* **276,** 13198–13208
29. Mancuso, D. J., Jenkins, C. M., and Gross, R. W. (2000) *J. Biol. Chem.* **275,** 9937–9945
30. Tanaka, H., Takeya, R., and Sumimoto, H. (2000) *Biochem. Biophys. Res. Commun.* **272,** 320–326
31. Ma, Z., Ramanadham, S., Kempe, K., Chi, X. S., Ladenson, J., and Turk, J. (1997) *J. Biol. Chem.* **272,** 11118–11127
32. Boilard, E., and Surette, M. E. (2001) *J. Biol. Chem.* **276,** 17568–17575
33. Isenović, E., and LaPointe, M. C. (2000) *Hypertension* **35,** 249–254
34. Maggi, L. B., Jr., Moran, J. M., Scarim, A. L., Ford, D. A., Yoon, J. W., McHowat, J., Buller, R. M., and Corbett, J. A. (2002) *J. Biol. Chem.* **277,** 38449–38455
35. Tithof, P. K., Olivero, J., Ruehle, K., and Ganey, P. E. (2000) *Toxicol. Sci.* **53,** 40–47
36. Williams, S. D., and Ford, D. A. (2001) *Am. J. Physiol. Heart Circ. Physiol.* **281,** H168–H176
37. Moran, J. M., Buller, R. M., McHowat, J., Turk, J., Wohltmann, M., Gross, R. W., and Corbett, J. A. (2005) *J. Biol. Chem.* **280,** 28162–28168
38. Ramanadham, S., Hsu, F. F., Bohrer, A., Ma, Z., and Turk, J. (1999) *J. Biol. Chem.* **274,** 13915–13927
39. Ramanadham, S., Song, H., Hsu, F. F., Zhang, S., Crankshaw, M., Grant, G. A., Newgard, C. B., Bao, S., Ma, Z., and Turk, J. (2003) *Biochemistry* **42,** 13929–13940
40. Ramanadham, S., Hsu, F. F., Zhang, S., Jin, C., Bohrer, A., Song, H., Bao, S., Ma, Z., and Turk, J. (2004) *Biochemistry* **43,** 918–930
41. Lei, X., Zhang, S., Bohrer, A., Bao, S., Song, H., and Ramanadham, S. (2007) *Biochemistry* **46,** 10170–10185
42. Lei, X., Zhang, S., Bohrer, A., and Ramanadham, S. (2008) *J. Biol. Chem.* **283,** 34819–34832
43. Nozaki, J., Kubota, H., Yoshida, H., Naitoh, M., Goji, J., Yoshinaga, T., Mori, K., Koizumi, A., and Nagata, K. (2004) *Genes Cells* **9,** 261–270
44. Kayo, T., and Koizumi, A. (1998) *J. Clin. Invest.* **101,** 2112–2118
45. Yoshioka, M., Kayo, T., Ikeda, T., and Koizumi, A. (1997) *Diabetes* **46,** 887–894
46. Miyazaki, J., Araki, K., Yamato, E., Ikegami, H., Asano, T., Shibasaki, Y., Oka, Y., and Yamamura, K. (1990) *Endocrinology* **127,** 126–132
47. Desagher, S., Osen-Sand, A., Nichols, A., Eskes, R., Montessuit, S., Lauper, S., Maundrell, K., Antonsson, B., and Martinou, J. C. (1999) *J. Cell Biol.*

144, 891–901
48. Sato, R., Yang, J., Wang, X., Evans, M. J., Ho, Y. K., Goldstein, J. L., and Brown, M. S. (1994) *J. Biol. Chem.* **269,** 17267–17273
49. Kim, J. B., and Spiegelman, B. M. (1996) *Genes Dev.* **10,** 1096–1107
50. Salvalaggio, P. R., Deng, S., Ariyan, C. E., Millet, I., Zawalich, W. S., Basadonna, G. P., and Rothstein, D. M. (2002) *Transplantation* **74,** 877–879
51. Yoshida, H. (2007) *FEBS J.* **274,** 630–658
52. Hsu, F. F., and Turk, J. (2000) *J. Am. Soc. Mass Spectrom.* **11,** 437–449
53. Seashols, S. J., del Castillo Olivares, A., Gil, G., and Barbour, S. E. (2004) *Biochim. Biophys. Acta* **1684,** 29–37
54. Wang, H., Kouri, G., and Wollheim, C. B. (2005) *J. Cell Sci.* **118,** 3905–3915
55. Furuta, E., Pai, S. K., Zhan, R., Bandyopadhyay, S., Watabe, M., Mo, Y. Y., Hirota, S., Hosobe, S., Tsukada, T., Miura, K., Kamada, S., Saito, K., Iiizumi, M., Liu, W., Ericsson, J., and Watabe, K. (2008) *Cancer Res.* **68,** 1003–1011
56. Menendez, J. A., and Lupu, R. (2007) *Nat. Rev. Cancer* **7,** 763–777
57. Porstmann, T., Griffiths, B., Chung, Y. L., Delpuech, O., Griffiths, J. R., Downward, J., and Schulze, A. (2005) *Oncogene* **24,** 6465–6481
58. Han, D., Lerner, A. G., Vande Walle, L., Upton, J. P., Xu, W., Hagen, A., Backes, B. J., Oakes, S. A., and Papa, F. R. (2009) *Cell* **138,** 562–575
59. Chipuk, J. E., Bouchier-Hayes, L., and Green, D. R. (2006) *Cell Death Differ.* **13,** 1396–1402
60. Garrido, C., Galluzzi, L., Brunet, M., Puig, P. E., Didelot, C., and Kroemer, G. (2006) *Cell Death Differ.* **13,** 1423–1433
61. Korsmeyer, S. J., Wei, M. C., Saito, M., Weiler, S., Oh, K. J., and Schlesinger, P. H. (2000) *Cell Death Differ.* **7,** 1166–1173
62. Schafer, Z. T., and Kornbluth, S. (2006) *Dev. Cell* **10,** 549–561
63. Wang, Z., Ramanadham, S., Ma, Z. A., Bao, S., Mancuso, D. J., Gross, R. W., and Turk, J. (2005) *J. Biol. Chem.* **280,** 6840–6849
64. Werstuck, G. H., Lentz, S. R., Dayal, S., Hossain, G. S., Sood, S. K., Shi, Y. Y., Zhou, J., Maeda, N., Krisans, S. K., Malinow, M. R., and Austin, R. C. (2001) *J. Clin. Invest.* **107,** 1263–1273
65. Ye, J., Rawson, R. B., Komuro, R., Chen, X., Davé, U. P., Prywes, R., Brown, M. S., and Goldstein, J. L. (2000) *Mol. Cell* **6,** 1355–1364
66. Brown, M. S., and Goldstein, J. L. (1997) *Cell* **89,** 331–340
67. Izumi, T., Yokota-Hashimoto, H., Zhao, S., Wang, J., Halban, P. A., and Takeuchi, T. (2003) *Diabetes* **52,** 409–416
68. Mathews, C. E., Langley, S. H., and Leiter, E. H. (2002) *Transplantation* **73,** 1333–1336
69. Ron, D. (2002) *J. Clin. Invest.* **109,** 443–445
70. Schmidt, R. E., Green, K. G., Snipes, L. L., and Feng, D. (2009) *Exp. Neurol.* **216,** 207–218

Pharmacology, Biochemistry and Behavior 92 (2009) 1–5

Contents lists available at ScienceDirect

Pharmacology, Biochemistry and Behavior

journal homepage: www.elsevier.com/locate/pharmbiochembeh

Levels of *N*-acylethanolamines in O,O,S-trimethylphosphorothioate (OOS-TMP)-treated C57BL/6J mice and potential anti-obesity, anti-diabetic effects of OOS-TMP in hyperphagia and hyperglycemia mouse models

Linfang Huang [a,b], Megumi Toyoshima [b], Akihiro Asakawa [b], Kayoko Inoue [b], Kouji Harada [b], Tomomi Kinoshita [c], Shilin Chen [a], Akio Koizumi [b,*]

[a] *Institute of Medicinal Plant Development, Chinese Academy of Medical Sciences & Peking Union Medical College, Beijing 1000193, China*
[b] *Department of Health and Environmental Sciences, Kyoto University Graduate School of Medicine, Kyoto 606-8501, Japan*
[c] *Graduate School of Engineering, Kyoto University, Kyoto 606-8510, Japan*

ARTICLE INFO

Article history:
Received 3 June 2008
Received in revised form 1 October 2008
Accepted 10 October 2008
Available online 1 November 2008

Keywords:
N-acylethanolamines
O,O,S-trimethylphosphorothioate
Anorexia
GC/MS
db/db mice
Akita mice
Anti-diabetic
Anti-obesity

ABSTRACT

O,O,S-Trimethylphosphorothioate (OOS-TMP) has been shown to induce hypophagia and hypopraxia. Recent studies suggest that OOS-TMP-induced anorexia is partly mediated by its effect on the central nervous system. In this study, we examined the profiles of *N*-acylethanolamines (NEAs), including five amide-linked compounds, in the gastrointestinal system in C57BL/6J (B6) mice. The present results shown an orexigenic profile of the levels of NEAs with downregulation of the anorectic lipid, *N*-stearoylethanolamine (SEA), upregulation of the orexigenic lipid, 2-arachidonoyl glycerol (2-AG), at 2 h and upregulation of 2-AG at 24 h albeit with significant anorexia. However, the data indicated that the high level of 2-AG may be responsible for the hypopraxia. We next explored whether OOS-TMP may affect two models of hyperphagia and hyperglycemia, *ins2*$^{+/Akita}$ B6 (Akita) and B6-*lepr*^{db}/*lepr*^{db} mice (db/db). We identified potential anorexigenic effects in B6, Akita and db/db mice. Moreover, OOS-TMP was found to reduce blood glucose in Akita mice but not in db/db mice. Collectively, these findings suggest that *N*-acylethanolamines are not involved in the hypophagia but rather hypopraxia, and may play multiple physiological roles in this process. OOS-TMP might be a promising candidate for anti-obesity and anti-diabetic drug development.

1. Introduction

O,O,S-trimethylphosphorothioate (OOS-TMP) is a contaminant in a number of widely used organophosphorous insecticides. It has been recognized as a unique environmental and lung toxicant that causes emaciation, lung injury, hypercapnia, hypothermia, hyperethanolaminuria and death owing to wasting without inhibition of AchE activity in mammalian species. (Koizumi et al., 1988; Aldridge et al., 1979; Verschoyle and Cabral, 1982; Imamura et al., 1983a,b; Aldridge et al., 1985; Gandy and Imamura, 1985; Umetsu et al., 1977).

Anorexia is one of the typical symptoms of the wasting syndrome caused by OOS-TMP administered by per os, intracerebroventricular (i.c.v.) or intraperitoneal (i.p.) routes, and is accompanied by hypothermia and hypopraxia (Huang et al., 2007; Ohtaka et al., 1995; Hasegawa and Koizumi, 1990).

Regulation of appetite and body weight is mediated by a complex physiological network involving both the central and peripheral nervous systems (Schwartz et al., 2000). In our previous study, both i.c.v. and i.p. injections transiently induced hypophagia at a dose of 5 mg/kg, with mild bronchial damages without alveolar injury. Hypophagia was accompanied by upregulation of corticotropin releasing factor (CRF) in the hypothalamus. At doses higher than 5 mg/kg, i.c.v. injection induced continuous hypophagia from 20 min to 72 h after dosing, accompanied by hypothermia and lung injury. OOS-TMP is thought to induce hypophagia by enhancing the expression of CRF in the hypothalamus (Huang et al., 2007). However, the role of the peripheral gastrointestinal system in hypophagia remains unclear.

N-acylethanolamines (NAEs) are a group of lipid mediator molecules with a wide range of biological effects. It is generally believed that they are formed from *N*-acylated phosphatidylethanolamines (NAPEs) (Schmid et al., 1990; Hansen et al., 2002; Schmid et al., 2002). Increasing evidence has demonstrated the ability of the *N*-acylethanolamines to control appetite, lipid homeostasis and energy balance. *N*-arachidonoylethanolamine (AEA), 2-arachidonoylglycerol (2-AG), *N*-palmitoylethanolamine (PEA), *N*-oleoylethanolamine (OEA) and *N*-stearoylethanolamine (SEA) belong

Abbreviations: OOS-TMP, O,O,S-trimethylphosphorothioate; i.c.v., intracerebroventricular; NEAs, *N*-acylethanolamines; PEA, *N*-palmitoylethanolamine; OEA, *N*-oleoylethanolamine; AEA, *N*-arachidonoylethanolamine (anandamide); 2-AG, 2-arachidonoyl glycerol; SEA, *N*-stearoylethanolamine; GC/MS, gas chromatography/mass spectrometry.

* Corresponding author. Department of Health and Environmental Sciences, Graduate School of Medicine, Kyoto University, Konoe-cho Yoshida Sakyo-ku Kyoto, 606-8501, Japan. Tel.: +81 75 753 4456; fax: +81 75 753 4458.
E-mail address: koizumi@pbh.med.kyoto-u.ac.jp (A. Koizumi).

0091-3057/$ – see front matter © 2008 Published by Elsevier Inc.
doi:10.1016/j.pbb.2008.10.003